Two-body non-leptonic heavy-to-heavy decays at NNLO in QCD factorization

Tobias Huber,[a] **Susanne Kränkl**[a] **and Xin-Qiang Li**[b]

[a]*Naturwissenschaftlich-Technische Fakultät,*
Universität Siegen, Walter-Flex-Str. 3, 57068 Siegen, Germany

[b]*Institute of Particle Physics and Key Laboratory of Quark and Lepton Physics (MOE),*
Central China Normal University, Wuhan, Hubei 430079, P.R. China

E-mail: huber@physik.uni-siegen.de, kraenkl@physik.uni-siegen.de,
xqli@itp.ac.cn

ABSTRACT: We evaluate in the framework of QCD factorization the two-loop vertex corrections to the decays $\bar{B}_{(s)} \to D_{(s)}^{(*)+} L^-$ and $\Lambda_b \to \Lambda_c^+ L^-$, where L is a light meson from the set $\{\pi, \rho, K^{(*)}, a_1\}$. These decays are paradigms of the QCD factorization approach since only the colour-allowed tree amplitude contributes at leading power. Hence they are sensitive to the size of power corrections once their leading-power perturbative expansion is under control. Here we compute the two-loop $\mathcal{O}(\alpha_s^2)$ correction to the leading-power hard scattering kernels, and give the results for the convoluted kernels almost completely analytically. Our newly computed contribution amounts to a positive shift of the magnitude of the tree amplitude by $\sim 2\%$. We then perform an extensive phenomenological analysis to NNLO in QCD factorization, using the most recent values for non-perturbative input parameters. Given the fact that the NNLO perturbative correction and updated values for form factors increase the theory prediction for branching ratios, while experimental central values have at the same time decreased, we reanalyze the role and potential size of power corrections by means of appropriately chosen ratios of decay channels.

KEYWORDS: Heavy Quark Physics, Perturbative QCD, Effective field theories

ARXIV EPRINT: 1606.02888

Contents

1 Introduction

Non-leptonic two-body decays of bottom mesons and baryons are interesting for phenomenological studies of the quark flavour sector of the Standard Model (SM) of particle physics. They yield observables like branching ratios and CP asymmetries that are relevant for studying the CKM mechanism of quark flavour mixing and allow access to the quantities of the unitarity triangle (cf. refs. [1–3]).

Oscillations and decays of B-mesons received considerable attention for the first time in the 1980s and 90s when the experiments ARGUS at DESY and CLEO at Cornell started to collect a lot of statistics. In the last decade, non-leptonic two-body $B_{(s)}$-decays have been extensively measured at the asymmetric e^+e^- colliders (B-factories) at SLAC and KEK, but also in hadronic environments such as the Tevatron, and the results obtained by the Babar, Belle, D0 and CDF collaborations have reached a high level of precision (see, e.g. [4]). In recent years the LHCb experiment at the LHC at CERN has become the main player as far as experimental physics of the bottom quark is concerned. A large data set on bottom mesons and baryons has been accumulated, and results related to non-leptonic

decays have been published (cf. [5, 6]) and further analyses are ongoing. In the near future also Belle II will contribute significantly to further improve the measurements [7].

With the plethora of precise experimental data on non-leptonic decays at hand, theoretical predictions at the same level of accuracy are very much desired. However, the theoretical description of non-leptonic two-body $B_{(s)}$ decays is notoriously complicated. A straightforward computation of the hadronic matrix elements which describe the weak transition is not feasible due to the presence of the strong interaction in the purely hadronic initial and final states. This circumstance entails QCD effects from many different scales which are, moreover, largely separated. In a first approach, known as naïve factorization, the hadronic transition matrix elements were factorized into a product of a form factor and a decay constant [8]. Subsequent studies built on flavour symmetries of the light quarks [9] and on factorization frameworks such as perturbative QCD (pQCD) [10, 11] and QCD factorization (QCDF) [12–14], to mention the most prominent ones. Certain combinations of these approaches can also be found (see e.g. [15]).

In the present work we adopt the QCDF framework and consider non-leptonic heavy-to-heavy transitions, which at the quark-level are mediated by the weak decay $b \to c\bar{u}d(s)$, where we treat the bottom and the charm quark as massive and the light quarks as massless. Performing an expansion of the amplitude in powers of $\Lambda_{\rm QCD}/m_b$, where $\Lambda_{\rm QCD}$ is the typical hadronic scale, a systematic separation of QCD effects from different scales can be achieved and corrections to naïve factorization be systematically included. Taking the decay $\bar{B} \to D^+ L^-$ as an example, the transition amplitude in the heavy-mass limit is then given by [13]

$$\langle D^+ L^- | \mathcal{Q}_i | \bar{B} \rangle = \sum_j F_j^{B \to D}(m_L^2) \int_0^1 du\, T_{ij}(u) \Phi_L(u) \,, \tag{1.1}$$

where the local four-fermion operators $\mathcal{Q}_i$ describe the underlying weak decay. The $F_j^{B \to D}$ form factors and the light-cone distribution amplitude (LCDA) Φ_L of the light meson contain long-distance effects and can be obtained from non-perturbative methods like QCD sum rules and lattice QCD. The hard-scattering kernels T_{ij}, on the other hand, only receive contributions from scales of $\mathcal{O}(m_b)$ and are accessible in a perturbative expansion in the strong coupling α_s. After the convolution over the momentum fraction u of the valence quark inside the light meson, they yield a perturbative contribution to the topological tree amplitude $a_1(D^+ L^-)$. Taking the decay $\bar{B} \to D^+ \pi^-$ as a specific example, the latter is defined via [13]

$$\mathcal{A}(\bar{B} \to D^+ \pi^-) = i \frac{G_F}{\sqrt{2}} V_{ud}^* V_{cb}\, a_1(D^+ \pi^-)\, f_\pi\, F_0^{B \to D}(m_\pi^2)\, (m_B^2 - m_D^2) \,. \tag{1.2}$$

The leading-power hard-scattering kernels have been known to next-to-leading order (NLO) accuracy for more than a decade for both heavy-to-light [12, 14, 16] and heavy-to-heavy [13] decays. In the latter case, expanding the LCDA in Gegenbauer moments up to the first moment α_1^L, the topological tree amplitude a_1 to NLO reads [13]

$$|a_1(\bar{B} \to D^+ L^-)| = (1.055^{+0.019}_{-0.017}) - (0.013^{+0.011}_{-0.006})\alpha_1^L \,,$$
$$|a_1(\bar{B} \to D^{*+} L^-)| = (1.054^{+0.018}_{-0.017}) - (0.015^{+0.013}_{-0.007})\alpha_1^L \,. \tag{1.3}$$

For the light meson being π or ρ we have $\alpha_1^{\pi(\rho)} = 0$ and for the kaon $|\alpha_1^K| < 1$ is assumed [13]. With this mild dependence on the light meson LCDA we encounter a quasi-universal value $|a_1| \simeq 1.05$ for heavy-to-heavy decays in QCDF to NLO accuracy. A quasi-universality was also found upon extracting a_1 from experimental data [17]. However, the favoured central value $|a_1| \simeq 0.95$ for the decays $\bar{B} \to D^{(*)+}L^-$ ($L = \pi$, K), with errors in the individual channels at the 10–20% level, is considerably lower.

In recent years next-to-next-to-leading order (NNLO) corrections to heavy-to-light decays have become available [18–31], and besides the prospects of increasing precision on the experimental side, there is multiple motivation to go beyond NLO in heavy-to-heavy transitions as well: first, the NLO correction is small since it is proportional to a small Wilson coefficient and, in addition, is colour-suppressed. At NNLO the colour suppression gets lifted and the large Wilson coefficient re-enters, and therefore the NNLO correction could be comparable in size to the NLO term. Moreover, it is interesting to see whether the quasi-universality of a_1 persists at NNLO. At leading power the decays $\bar{B}_{(s)} \to D_{(s)}^{(*)+}L^-$ receive only vertex corrections to the colour-allowed tree topology. Interactions with the spectator quark as well as the weak annihilation topology are power-suppressed [13] and there are neither contributions from penguin operators nor is there a colour-suppressed tree topology. Therefore, a precise knowledge of the colour-allowed tree amplitude a_1 allows to reliably estimate the size of power corrections to eq. (1.1) by comparison to experimental data, and at the same time provides a test of the QCDF framework. This requires that the perturbative expansion of the hard scattering kernel is under control, and that also the uncertainties of the non-perturbative input parameters (form factors, decay constants, LCDAs) can be minimized. In the present work we therefore calculate the two-loop vertex correction to the leading-power hard scattering kernels in the framework of QCDF. Parts of the computational procedure were already presented in [32, 33]. Here, we give the full result of the technically challenging two-loop calculation. Besides, we present an updated phenomenological analysis of $\bar{B}_{(s)} \to D_{(s)}^{(*)+}L^-$ decays, with a light meson from the set $L = \{\pi, \rho, K^{(*)}, a_1\}$,[1] using the most recent values for non-perturbative input parameters (for another recent analysis, see [34]).

Recently, non-leptonic Λ_b decays have received considerable attention as well. Data on $\Lambda_b \to \Lambda_c^+ L^-$ with L being π or K [35] and on baryonic form factors have become available [36]. Therefore, we extend our study to these decays. Factorization has not yet been systematically established for baryonic decays, but was discussed in ref. [37]. As a systematic derivation of the baryonic factorization formula is beyond the scope of this work we adopt the factorization formula eq. (4) of ref. [37], with appropriate modifications to take perturbative corrections into account.

This article is organized as follows: in section 2 we present our theoretical framework by specifying our operator basis in the effective weak Hamiltonian. Subsequently, we derive the master formulas for the hard scattering kernels by performing a matching onto Soft-Collinear Effective Theory. In section 3 we discuss the calculation of the two-loop Feynman

---

[1]We use the same symbol a_1 for both, the meson $a_1(1260)$ and the colour-allowed tree amplitude $a_1(D^+L^-)$. We think that in each case it is clear from the context which quantity we refer to.

diagrams and specify the input to the master formulas. The analytical results of the hard scattering kernels after the convolution with the LCDAs are presented in section 4. In section 5 we give the formulas for converting from the pole to the $\overline{\text{MS}}$ scheme for the b- and c-quark masses. We present the results of our extensive phenomenological analysis in section 6, and conclude in section 7.

2 Theoretical framework

2.1 Five-flavour theory

We work in the effective five-flavour theory where the top quark, the heavy gauge bosons $W^\pm$, Z^0 and the Higgs boson are integrated out and their effects are absorbed into short-distance Wilson coefficients. The decays $\bar{B}_{(s)} \to D_{(s)}^{(*)+} L^-$ and $\Lambda_b \to \Lambda_c^+ L^-$ are mediated at parton level by a $b \to c\bar{u}d(s)$ transition for $L = \pi, \rho, a_1 (K, K^*)$. The corresponding QCD amplitude is computed in the framework of the effective weak Hamiltonian [14, 38], which for the problem at hand simply reads

$$\mathcal{H}_{\text{eff}} = \frac{G_F}{\sqrt{2}} V_{cb} V_{ud}^* \left(C_1 \mathcal{Q}_1 + C_2 \mathcal{Q}_2 \right) + \text{h.c.}. \tag{2.1}$$

We restrict our notation to the case of a $b \to c\bar{u}d$ transition. The expressions for a strange quark in the final state are obtained by obvious replacements. The local current-current operators in the Chetyrkin-Misiak-Münz (CMM) basis [39, 40] read

$$\mathcal{Q}_1 = \bar{c}\gamma^\mu(1-\gamma_5)T^A b \ \ \bar{d}\gamma_\mu(1-\gamma_5)T^A u \,, \tag{2.2}$$

$$\mathcal{Q}_2 = \bar{c}\gamma^\mu(1-\gamma_5)b \ \ \bar{d}\gamma_\mu(1-\gamma_5)u \,, \tag{2.3}$$

where $\mathcal{Q}_1$ and $\mathcal{Q}_2$ are referred to as colour-octet and colour-singlet operator, respectively. The use of the CMM basis allows for a consistent treatment of γ_5 in the naïve dimensional regularization scheme with fully anti-commuting γ_5.

Moreover, as the computation will be performed in dimensional regularization, we have to augment our physical operators $\mathcal{Q}_{1,2}$ by a set of evanescent operators, for which we adopt the convention [41, 42]

$$E_1^{(1)} = \left[\bar{c}\gamma^\mu\gamma^\nu\gamma^\rho(1-\gamma_5)T^A b \right] \left[\bar{d}\gamma_\mu\gamma_\nu\gamma_\rho(1-\gamma_5)T^A u \right] - 16\mathcal{Q}_1 \,, \tag{2.4}$$

$$E_2^{(1)} = \left[\bar{c}\gamma^\mu\gamma^\nu\gamma^\rho(1-\gamma_5)b \right] \left[\bar{d}\gamma_\mu\gamma_\nu\gamma_\rho(1-\gamma_5)u \right] - 16\mathcal{Q}_2 \,, \tag{2.5}$$

$$E_1^{(2)} = \left[\bar{c}\gamma^\mu\gamma^\nu\gamma^\rho\gamma^\sigma\gamma^\lambda(1-\gamma_5)T^A b \right] \left[\bar{d}\gamma_\mu\gamma_\nu\gamma_\rho\gamma_\sigma\gamma_\lambda(1-\gamma_5)T^A u \right] - 20E_1^{(1)} - 256\mathcal{Q}_1 \,, \tag{2.6}$$

$$E_2^{(2)} = \left[\bar{c}\gamma^\mu\gamma^\nu\gamma^\rho\gamma^\sigma\gamma^\lambda(1-\gamma_5)b \right] \left[\bar{d}\gamma_\mu\gamma_\nu\gamma_\rho\gamma_\sigma\gamma_\lambda(1-\gamma_5)u \right] - 20E_2^{(1)} - 256\mathcal{Q}_2 \,. \tag{2.7}$$

These unphysical operators vanish in $D = 4$ dimensions but contribute if $D \neq 4$ since they mix under renormalization with the physical operators. At two-loop accuracy the set of operators (2.2)–(2.7) closes under renormalization.

2.2 Matching onto SCET and master formulas

We construct the master formulas for the hard scattering kernels by performing a matching from the effective weak Hamiltonian[2] onto Soft-Collinear Effective Theory (SCET) with

---

[2]In the following we refer to this side of the matching equation as the QCD side.
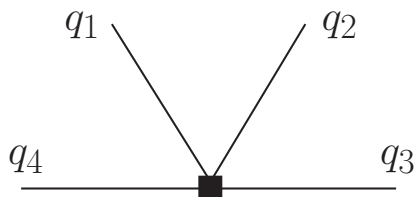
Figure 1. The tree-level Feynman diagram for the $b \to c\bar{u}d$ transition in full (five flavour) QCD: the black square represents the vertex of the effective weak interaction. The momenta q_4 and q_3 belong to the quark lines with masses m_b and m_c, respectively, and $q_1 + q_2 = q$ is the momentum of the light meson. All momenta are taken to be incoming.

three light flavours. The procedure follows similar lines than the derivation of the master formulas for the hard kernels in heavy-to-light transitions [28].

The kinematics of the $b \to c\bar{u}d$ transition is shown in the tree-level Feynman diagram depicted in figure 1. The b and the c quark are considered to be massive and carry momenta q_4 and q_3, respectively. The massless d and $\bar{u}$ quarks share the momentum q with $q_1 = uq$ and $q_2 = (1-u)q \equiv \bar{u}q$, where $u \in [0,1]$ is the momentum fraction of the valence quark inside the light meson. All external momenta are taken to be incoming and are subject to the on-shell constraints $q_4^2 = m_b^2$, $q_3^2 = m_c^2$, and $q^2 = 0$.

We consider a reference frame in which the b quark within the B meson moves with momentum $q_b = m_b v + k$, where k is a residual momentum of order of the typical hadronic scale Λ_{QCD}, and v is the velocity of the B meson. The b quark can then be described by a heavy-quark field h_v which satisfies the equation of motion $\slashed{v} h_v = h_v$. We further choose a reference frame such that the energetic light meson moves in the light-cone direction n_+. The light-like vectors n_+ and $n_- = 2v - n_+$ then fulfill the constraints $n_\pm^2 = 0$ and $n_+ n_- = 2$. As the quark and the anti-quark in the light meson nearly move in the same direction we can describe them by the same type of collinear SCET field χ, which satisfies the equations of motion $\slashed{n}_+ \chi = 0$ and $\bar{\chi}\slashed{n}_+ = 0$. In the derivation of the factorization formula (1.1) the power counting $m_c/m_b \sim \mathcal{O}(1)$ was adopted. Hence, we treat the charm quark as a heavy quark and consequently describe it — in analogy to the b quark — by another heavy-quark field $h_{v'}$ with velocity v' and equation of motion $\slashed{v}' h_{v'} = h_{v'}$.

The amplitudes in full QCD and in SCET are made equal by adjusting the corresponding hard coefficients at the matching scale. We express the renormalized matrix elements of the QCD operators (2.2) and (2.3) as a linear combination of a basis of SCET operators,

$$\langle \mathcal{Q}_i \rangle = \sum_{a=1}^{3} \left[H_{ia} \langle \mathcal{O}_a \rangle + H'_{ia} \langle \mathcal{O}'_a \rangle \right] , \tag{2.8}$$

where H_{ia} and H'_{ia} are the matching coefficients. The basis of SCET operators is given by

$$\mathcal{O}_1 = \bar{\chi} \frac{\slashed{n}_-}{2}(1-\gamma_5)\chi \ \ \bar{h}_{v'}\slashed{n}_+(1-\gamma_5)h_v , \tag{2.9}$$

$$\mathcal{O}_2 = \bar{\chi} \frac{\slashed{n}_-}{2}(1-\gamma_5)\gamma_\perp^\alpha \gamma_\perp^\beta \chi \ \ \bar{h}_{v'}\slashed{n}_+(1-\gamma_5)\gamma_{\perp\beta}\gamma_{\perp\alpha}h_v , \tag{2.10}$$

$$\mathcal{O}_3 = \bar{\chi}\frac{\slashed{n}_-}{2}(1-\gamma_5)\gamma_\perp^\alpha\gamma_\perp^\beta\gamma_\perp^\gamma\gamma_\perp^\delta\chi \ \ \bar{h}_{v'}\slashed{n}_+(1-\gamma_5)\gamma_{\perp\delta}\gamma_{\perp\gamma}\gamma_{\perp\beta}\gamma_{\perp\alpha}h_v\,, \tag{2.11}$$

$$\mathcal{O}'_1 = \bar{\chi}\frac{\slashed{n}_-}{2}(1-\gamma_5)\chi \ \ \bar{h}_{v'}\slashed{n}_+(1+\gamma_5)h_v\,, \tag{2.12}$$

$$\mathcal{O}'_2 = \bar{\chi}\frac{\slashed{n}_-}{2}(1-\gamma_5)\gamma_\perp^\alpha\gamma_\perp^\beta\chi \ \ \bar{h}_{v'}\slashed{n}_+(1+\gamma_5)\gamma_{\perp\alpha}\gamma_{\perp\beta}h_v\,, \tag{2.13}$$

$$\mathcal{O}'_3 = \bar{\chi}\frac{\slashed{n}_-}{2}(1-\gamma_5)\gamma_\perp^\alpha\gamma_\perp^\beta\gamma_\perp^\gamma\gamma_\perp^\delta\chi \ \ \bar{h}_{v'}\slashed{n}_+(1+\gamma_5)\gamma_{\perp\alpha}\gamma_{\perp\beta}\gamma_{\perp\gamma}\gamma_{\perp\delta}h_v\,. \tag{2.14}$$

Here, the perpendicular component of a Dirac matrix is defined by

$$\gamma^\mu = \slashed{n}_+\frac{n_-^\mu}{2} + \slashed{n}_-\frac{n_+^\mu}{2} + \gamma_\perp^\mu. \tag{2.15}$$

Moreover, we have omitted the Wilson lines which render the non-local light currents $\bar{\chi}(tn_-)[\ldots]\chi(0)$ gauge invariant. One therefore has to keep in mind that the coefficients H_{ia} are also functions of the variable t, and the products $H_{ia}^{(\prime)}\langle\mathcal{O}_a^{(\prime)}\rangle$ in eq. (2.8) are in fact convolutions. We also remark that the SCET operator basis is chosen such that all operators with index $a > 1$ are evanescent, and we have the two physical SCET operators $\mathcal{O}_1$ and $\mathcal{O}'_1$. The operators (2.9)–(2.11) have the same structure as those in [28] for heavy-to-light transitions, but with a heavy-quark field $h_{v'}$ instead of an anti-collinear SCET field ξ in direction n_-. For heavy-to-heavy transitions this set of operators has to be extended by those in (2.12)–(2.14) which have a different chirality structure, to take into account the non-vanishing mass of the charm quark. For technical details on the operators see [19, 43].

We first consider the expansion of the left-hand side of eq. (2.8) in terms of on-shell QCD amplitudes. The expression for the renormalized matrix elements reads

$$
\begin{aligned}
\langle \mathcal{Q}_i \rangle = &\left\{ A_{ia}^{(0)} + \frac{\alpha_s}{4\pi}\left[A_{ia}^{(1)} + Z_{\text{ext}}^{(1)}A_{ia}^{(0)} + Z_{ij}^{(1)}A_{ja}^{(0)} \right] \right.\\
&+ \left(\frac{\alpha_s}{4\pi}\right)^2 \left[A_{ia}^{(2)} + Z_{ij}^{(1)}A_{ja}^{(1)} + Z_{ij}^{(2)}A_{ja}^{(0)} + Z_{\text{ext}}^{(1)}A_{ia}^{(1)} + Z_{\text{ext}}^{(2)}A_{ia}^{(0)} + Z_{\text{ext}}^{(1)}Z_{ij}^{(1)}A_{ja}^{(0)} \right.\\
&\left.+ (-i)\delta m_b^{(1)} A_{ia}^{*(1)} + (-i)\delta m_c^{(1)} A_{ia}^{**(1)} + Z_\alpha^{(1)}A_{ia}^{(1)} \right] + \mathcal{O}(\alpha_s^3) \left.\right\}\langle\mathcal{O}_a\rangle^{(0)}\\
&+ (A \leftrightarrow A')\langle\mathcal{O}'_a\rangle^{(0)}\quad.
\end{aligned} \tag{2.16}
$$

Here, a sum over $a = 1, 2, 3$ is understood, and α_s is the $\overline{\text{MS}}$ strong coupling constant with five active flavours. The index $i = 1, 2$ denotes the physical operators from (2.2) and (2.3) only, whereas j includes physical as well as evanescent operators from (2.2)–(2.7), hence $j = 1, \ldots, 6$. The $A^{(l)}$ are the bare l-loop on-shell amplitudes and $A^{*(1)}$ ($A^{**(1)}$) is the one-loop bare on-shell amplitude with a b (c) quark mass insertion on the heavy b (c) line. The primed amplitudes are defined analogously. The renormalization factors Z_{ij}, Z_{ext} and Z_α stem from operator renormalization, wave-function renormalization of all external legs and coupling renormalization, respectively. They are defined in a perturbative expansion

$$Z = 1 + \sum_{k=1}^\infty \left(\frac{\alpha_s}{4\pi}\right)^k Z^{(k)}\,. \tag{2.17}$$

The operator renormalization is performed in the $\overline{\text{MS}}$ scheme, whereas for the mass and the wave-function renormalization the on-shell scheme is applied. Renormalized matrix elements of evanescent operators vanish also beyond tree level. Nevertheless, these operators cannot be neglected right from the beginning as they yield physical contributions to the products $Z_{ij}^{(1)} A_{ja}^{(0)}$, $Z_{ij}^{(1)} A_{ja}^{(1)}$, and $Z_{ij}^{(2)} A_{ja}^{(0)}$.

Similarly, we can write down the expression for the renormalized matrix elements of the SCET operators that enter the right-hand side of eq. (2.8) and obtain

$$
\begin{aligned}
\langle \mathcal{O}_a \rangle = \Big\{ & \delta_{ab} + \frac{\hat{\alpha}_s}{4\pi} \left[M_{ab}^{(1)} + Y_{\text{ext}}^{(1)} \delta_{ab} + Y_{ab}^{(1)} \right] \\
& + \left(\frac{\hat{\alpha}_s}{4\pi} \right)^2 \left[M_{ab}^{(2)} + Y_{\text{ext}}^{(1)} M_{ab}^{(1)} + Y_{ac}^{(1)} M_{cb}^{(1)} + \hat{Z}_\alpha^{(1)} M_{ab}^{(1)} + Y_{\text{ext}}^{(2)} \delta_{ab} \right. \\
& \left. + Y_{\text{ext}}^{(1)} Y_{ab}^{(1)} + Y_{ab}^{(2)} \right] + \mathcal{O}\big(\hat{\alpha}_s^3\big) \Big\} \langle \mathcal{O}_b \rangle^{(0)} .
\end{aligned}
\tag{2.18}
$$

Here, $a = 1, 2, 3$ and a sum over $b = 1, 2, 3$ is understood. The $\overline{\text{MS}}$ strong coupling constant $\hat{\alpha}_s$ has three light flavours and $M^{(l)}$ are the bare l-loop SCET amplitudes. The $Y_{\text{ext}}^{(l)}$, $Y_{ab}^{(l)}$ and $\hat{Z}_\alpha^{(l)}$ are the l-loop wave-function, operator and coupling renormalization constants, respectively. They are defined in a perturbative expansion analogous to eq. (2.17) except that the strong coupling has only three light flavours. The corresponding expression for the primed operators from eqs. (2.12)–(2.14) is given by substituting $M \to M'$ and $\mathcal{O} \to \mathcal{O}'$ in eq. (2.18).

Eq. (2.18) can be simplified to a large extent. In dimensional regularization the on-shell renormalization constants Y_{ext} are equal to unity. Moreover, the bare on-shell amplitudes only contain scaleless integrals, which vanish in dimensional regularization. We thus arrive at the following simplified expression of eq. (2.18)

$$
\langle \mathcal{O}_a \rangle = \left\{ \delta_{ab} + \frac{\hat{\alpha}_s}{4\pi} Y_{ab}^{(1)} + \left(\frac{\hat{\alpha}_s}{4\pi} \right)^2 Y_{ab}^{(2)} + \mathcal{O}\big(\hat{\alpha}_s^3\big) \right\} \langle \mathcal{O}_b \rangle^{(0)} ,
\tag{2.19}
$$

which for the primed operators takes a similar form.

For relating the matching coefficients H_{ia} and H'_{ia} in eq. (2.8) to the hard scattering kernels we introduce two factorized QCD operators

$$
\mathcal{Q}^{(')\text{QCD}} = \left[\bar{q} \frac{\slashed{n}_-}{2}(1 - \gamma_5) q \right] \left[\bar{c} \slashed{n}_+ (1 \mp \gamma_5) b \right] ,
\tag{2.20}
$$

which are by definition the products of the two currents in brackets. The upper sign corresponds to the un-primed operator. The renormalized operators $\mathcal{Q}^{(')\text{QCD}}$ are then matched onto the renormalized SCET operators $\mathcal{O}_1$ and $\mathcal{O}'_1$ by adjusting the corresponding hard coefficients. This can be done separately for the light-to-light and heavy-to-heavy currents. For the renormalized light-to-light current we make the ansatz

$$
\left[\bar{q} \frac{\slashed{n}_-}{2}(1 - \gamma_5) q \right] = C_{\bar{q}q} \left[\bar{\chi} \frac{\slashed{n}_-}{2}(1 - \gamma_5) \chi \right] .
\tag{2.21}
$$

The heavy-to-heavy currents with different chiralities mix in the matching. Thus, we make the ansatz

$$\left[\bar{c}\, \slashed{n}_+(1-\gamma_5)b\right] = C_{FF}^{\mathrm{LL}}\left[\bar{h}_{v'}\slashed{n}_+(1-\gamma_5)h_v\right] + C_{FF}^{\mathrm{LR}}\left[\bar{h}_{v'}\slashed{n}_+(1+\gamma_5)h_v\right], \tag{2.22}$$

$$\left[\bar{c}\, \slashed{n}_+(1+\gamma_5)b\right] = C_{FF}^{\mathrm{RL}}\left[\bar{h}_{v'}\slashed{n}_+(1-\gamma_5)h_v\right] + C_{FF}^{\mathrm{RR}}\left[\bar{h}_{v'}\slashed{n}_+(1+\gamma_5)h_v\right]. \tag{2.23}$$

Since these equations are symmetric under interchanging $P_L \leftrightarrow P_R$ we have $C_{FF}^{\mathrm{LL}} = C_{FF}^{\mathrm{RR}} \equiv C_{FF}^{\mathrm{D}}$ and $C_{FF}^{\mathrm{LR}} = C_{FF}^{\mathrm{RL}} \equiv C_{FF}^{\mathrm{ND}}$. Finally, we obtain

$$\mathcal{Q}^{\mathrm{QCD}} = \left[\bar{q}\frac{\slashed{n}_-}{2}(1-\gamma_5)q\right]\left[\bar{c}\, \slashed{n}_+(1-\gamma_5)b\right] = C_{\bar{q}q}C_{FF}^{\mathrm{D}}\mathcal{O}_1 + C_{\bar{q}q}C_{FF}^{\mathrm{ND}}\mathcal{O}_1', \tag{2.24}$$

$$\mathcal{Q}'^{\mathrm{QCD}} = \left[\bar{q}\frac{\slashed{n}_-}{2}(1-\gamma_5)q\right]\left[\bar{c}\, \slashed{n}_+(1+\gamma_5)b\right] = C_{\bar{q}q}C_{FF}^{\mathrm{ND}}\mathcal{O}_1 + C_{\bar{q}q}C_{FF}^{\mathrm{D}}\mathcal{O}_1'. \tag{2.25}$$

Since by construction $\mathcal{Q}^{\mathrm{QCD}}$ and $\mathcal{Q}'^{\mathrm{QCD}}$ factorize into a light-to-light and a heavy-to-heavy current, the matrix element of these operators is the product of an LCDA and the full QCD form factor with the corresponding helicity structure.

We now consider the two hard scattering kernels $\hat{T}_i$ and $\hat{T}_i'$ that are defined by the following expression

$$\langle\mathcal{Q}_i\rangle = \hat{T}_i\langle\mathcal{Q}^{\mathrm{QCD}}\rangle + \hat{T}_i'\langle\mathcal{Q}'^{\mathrm{QCD}}\rangle + \sum_{a>1}\left[H_{ia}\langle\mathcal{O}_a\rangle + H_{ia}'\langle\mathcal{O}_a'\rangle\right]. \tag{2.26}$$

Comparing eqs. (2.8) and (2.26), $\hat{T}_i$ and $\hat{T}_i'$ can be related to the matching coefficients as follows

$$\begin{pmatrix}\hat{T}_i \\ \hat{T}_i'\end{pmatrix} = \begin{pmatrix} C_{\bar{q}q}C_{FF}^{\mathrm{D}} & C_{\bar{q}q}C_{FF}^{\mathrm{ND}} \\ C_{\bar{q}q}C_{FF}^{\mathrm{ND}} & C_{\bar{q}q}C_{FF}^{\mathrm{D}} \end{pmatrix}^{-1}\begin{pmatrix}H_{i1} \\ H_{i1}'\end{pmatrix}. \tag{2.27}$$

Plugging in the matching coefficients as expansions in the five-flavour coupling α_s, the matrix can be inverted order-by-order in α_s. We remark that $C_{\bar{q}q} = 1 + \mathcal{O}(\alpha_s^2)$, i.e. it receives a correction at two loops only since at one loop only scaleless integrals contribute. The explicit one-loop expressions for the heavy-to-heavy coefficients will be derived in section 3. For the diagonal coefficients we have $C_{FF}^{\mathrm{D}} = 1 + \mathcal{O}(\alpha_s)$. In contrast, the non-diagonal matching coefficients C_{FF}^{ND} that induce the chirality mixing only arise beyond tree level, $C_{FF}^{\mathrm{ND}} = \mathcal{O}(\alpha_s)$.

Putting everything together, the master formulas for the hard scattering kernels read

$$\hat{T}_i^{(0)} = A_{i1}^{(0)}$$

$$\hat{T}_i^{(1)} = A_{i1}^{(1)nf} + Z_{ij}^{(1)}A_{j1}^{(0)}$$

$$\hat{T}_i^{(2)} = A_{i1}^{(2)nf} + Z_{ij}^{(1)}A_{j1}^{(1)} + Z_{ij}^{(2)}A_{j1}^{(0)} + Z_{\alpha}^{(1)}A_{i1}^{(1)nf} - \hat{T}_i^{(1)}\left[C_{FF}^{\mathrm{D}(1)} + Y_{11}^{(1)} - Z_{\mathrm{ext}}^{(1)}\right]$$

$$\qquad - C_{FF}^{\mathrm{ND}(1)}\hat{T}_i'^{(1)} + (-i)\delta m_b^{(1)}A_{i1}^{*(1)nf} + (-i)\delta m_c^{(1)}A_{i1}^{**(1)nf} - \sum_{b\neq 1}H_{ib}^{(1)}Y_{b1}^{(1)}. \tag{2.28}$$
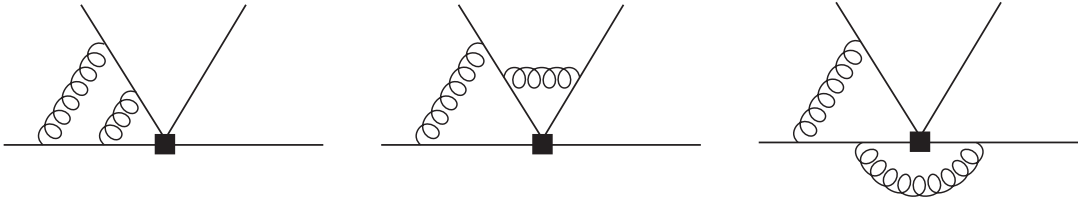
Figure 2. Sample of Feynman diagrams that contribute to the two-loop hard scattering kernels.

The expression for the primed kernels $\hat{T}'_i$ is given by eq. (2.28) with the replacement $A \leftrightarrow A'$, $H \leftrightarrow H'$, $\hat{T} \leftrightarrow \hat{T}'$. Note that the quantities $H^{(l)}$, $A^{(l)}$ and the hard kernels $\hat{T}^{(l)}$ depend on the quark mass ratio $z_c = m_c^2/m_b^2$ and the momentum fraction u of the quark inside the light meson (as do the corresponding primed quantities). Whenever they appear alongside a renormalization factor $Y^{(l)}$ such as $H_{ib}^{(1)}Y_{b1}^{(1)}$ we must keep in mind that these expressions must be interpreted as a convolution product $\int_0^1 du' \, H_{ib}^{(1)}(z_c, u')Y_{b1}^{(1)}(u', u)$.

The amplitudes $A_{i1}^{(l)nf}$ in eq. (2.28) are termed "non-factorizable". At one-loop the corresponding amplitudes are given by all Feynman diagrams with one gluon connecting the heavy and the light current. The one-loop Feynman diagrams where the gluon is attached solely to either the light or the heavy current are part of the LCDA and the form factor, respectively. The Feynman diagrams contributing to $A_{i1}^{(2)nf}$ can be found in figures 15 and 16 of ref. [13] and in addition include the one-loop self-energy insertions to the "non-factorizable" one-loop amplitudes. A sample of two-loop diagrams is shown in figure 2. $A_{i1}^{(2)nf}$ is technically the most challenging contribution to the two-loop kernels. Therefore, we briefly describe their evaluation in the next section and, moreover, specify the remaining input to eq. (2.28). The final expression of the hard scattering kernels must be free of ultraviolet and infrared divergences. We comment on this at the end of the next section.

Finally, we remark that eq. (2.28) has a structure similar to the corresponding expressions for the two-loop hard scattering kernel in the right-insertion contribution to the decay $B \to \pi\pi$, which is given in eq. (24) in [28]. The main difference is three-fold: first, we find two contributions $\hat{T}$ and $\hat{T}'$ to the hard scattering kernel as a result of the extended operator basis. Second, we encounter the off-diagonal element $C_{FF}^{\mathrm{ND}(1)}\hat{T}_1'^{(1)}$ due to the mixing of the heavy-to-heavy currents with different chirality structures. Finally, we have a mass counterterm for the massive charm quark in eq. (2.28).

3 Computational details

3.1 Technical aspects of the two-loop computation

We work in dimensional regularization with $D = 4 - 2\epsilon$ and expand the amplitudes in the parameter ϵ. The Feynman diagrams contributing to the bare two-loop amplitude $A^{(2)nf}$ then contain up to $1/\epsilon^4$ poles stemming from ultraviolet (UV) and infrared (IR) regions. We calculated them by applying commonly-used multi-loop techniques, including a new method for evaluating the master integrals. The procedure goes as follows: first, we decompose

all tensor integrals into scalar ones by applying the Passarino-Veltman decomposition [44]. We then perform the reduction of the Dirac structures to the SCET operator basis given in eqs. (2.9)–(2.14) in `Mathematica` by using simple algebraic transformations. The number of remaining scalar two-loop integrals exceeds several thousands and can be simplified by using the Laporta algorithm [45, 46], which is based on integration-by-parts identities [47]. Here, we apply the implementations AIR [48] (in `Maple`) and FIRE [49] (in `Mathematica`) of this algorithm to reduce the large number of integrals to a small set of master integrals. Many of the latter are already known from several $B \to \pi\pi$ calculations [25, 26, 28]. In addition, we find 23 yet unknown two-loop master integrals. Since most of them depend on two scales (the momentum fraction u and the quark-mass ratio $z_c = m_c^2/m_b^2$), an analytic solution by common techniques is hardly feasible. We therefore evaluate them by applying the approach of differential equations in a canonical basis recently advocated in [50]. The solution is given by iterated integrals and falls into the class of Goncharov polylogarithms [51]. We obtain analytic results for all 23 master integrals. Details on their calculation and the result of all master integrals can be found in [33].

3.2 Input to the master formulas

Here we give the explicit expressions for the renormalization factors and matching coefficients that enter the master formula, and in the end comment on the cancellation of the poles in ϵ once all pieces of the master formula are plugged in.

The operator renormalization factors Z_{ij} of the effective weak Hamiltonian were calculated to two-loop accuracy in the $\overline{\text{MS}}$ scheme in [41, 42]. The explicit one- and two-loop expressions read

$$Z^{(1)} = \frac{1}{\epsilon} \begin{pmatrix} -2 & \frac{4}{3} & \frac{5}{12} & \frac{2}{9} & 0 & 0 \\ 6 & 0 & 1 & 0 & 0 & 0 \end{pmatrix}, \tag{3.1}$$

$$Z^{(2)} = \frac{1}{\epsilon^2} \begin{pmatrix} 17 - \frac{4n_f T_f}{3} & \frac{2}{9}(4n_f T_f - 39) & \frac{5}{18}(n_f T_f - 15) & \frac{1}{54}(8n_f T_f - 93) & \frac{19}{96} & \frac{5}{108} \\ 4n_f T_f - 39 & 4 & \frac{2n_f T_f}{3} - \frac{31}{4} & 0 & \frac{5}{24} & \frac{1}{9} \end{pmatrix}$$

$$+ \frac{1}{\epsilon} \begin{pmatrix} \frac{8n_f T_f}{9} + \frac{79}{12} & \frac{20n_f T_f}{27} - \frac{205}{18} & \frac{1531}{288} - \frac{5n_f T_f}{108} & -\frac{2n_f T_f}{81} - \frac{1}{72} & \frac{1}{384} & -\frac{35}{864} \\ \frac{10n_f T_f}{3} + \frac{83}{4} & 3 & \frac{119}{16} - \frac{n_f T_f}{9} & \frac{8}{9} & -\frac{35}{192} & -\frac{7}{72} \end{pmatrix}. \tag{3.2}$$

Here, $n_f = 5$ is the total number of active quark flavours and $T_f = 1/2$. The row index of these matrices corresponds to $(\mathcal{Q}_1, \mathcal{Q}_2, E_1^{(1)}, E_2^{(1)}, E_1^{(2)}, E_2^{(2)})$ and the column index to $(\mathcal{Q}_1, \mathcal{Q}_2)$. The strong coupling constant is renormalized in the $\overline{\text{MS}}$ scheme as well, whereas the renormalization of the masses and the wave-functions is performed in the on-shell scheme. The corresponding renormalization factors are well known and shall not be repeated here.

In eq. (2.28) we further encounter the SCET operator renormalization factor Y_{11} that can be split into the following two parts

$$Y_{11}(u', u) = Z_{Jh}\delta(u - u') + Z_{\text{BL}}(u', u). \tag{3.3}$$

Here, Z_{Jh} and Z_{BL} are the renormalization factors for the HQET heavy-to-heavy and the SCET light-to-light current, respectively. Since one collinear sector in SCET is equivalent to full QCD, the renormalization constant Z_{BL} coincides with the ERBL kernel in QCD [52, 53]. We take Z_{BL} from [54], which for pseudoscalar and longitudinally polarized vector mesons reads

$$Z_{\mathrm{BL}}(v,w) = \delta(v-w) - \frac{\alpha_s}{4\pi}\frac{2C_F}{\epsilon}\left\{\frac{1}{w\bar{w}}\left[v\bar{w}\,\frac{\Theta(w-v)}{w-v} + w\bar{v}\,\frac{\Theta(v-w)}{v-w}\right]_+ - \frac{1}{2}\delta(v-w)\right.$$
$$\left. + \left[\frac{v}{w}\Theta(w-v) + \frac{\bar{v}}{\bar{w}}\Theta(v-w)\right]\right\} + \mathcal{O}(\alpha_s^2). \qquad (3.4)$$

The plus-distribution for symmetric kernels f is defined as follows,

$$\int dw\,[f(v,w)]_+\,g(w) = \int dw f(v,w)\,[g(w) - g(v)]. \qquad (3.5)$$

The renormalization factor Z_{Jh} can be obtained in a matching of the heavy-to-heavy QCD current $\bar{c}\,\slashed{n}_+(1-\gamma_5)b$ to the HQET current $\bar{h}_{v'}\slashed{n}_+(1-\gamma_5)h_v$. In this process also the matching coefficients C_{FF} can be determined. Beyond tree-level the QCD current also mixes into the chirality-flipped HQET current $\bar{h}_{v'}\slashed{n}_+(1+\gamma_5)h_v$. Hence, we make the following ansatz for the renormalized currents

$$\bar{c}\,\slashed{n}_+(1\mp\gamma_5)b = C_{FF}^{\mathrm{D}}\left[\bar{h}_{v'}\slashed{n}_+(1\mp\gamma_5)h_v\right] + C_{FF}^{\mathrm{ND}}\left[\bar{h}_{v'}\slashed{n}_+(1\pm\gamma_5)h_v\right], \qquad (3.6)$$

where we have already made use of the fact that both equations are symmetric under interchanging $P_L \leftrightarrow P_R$. The renormalization factor Z_{Jh} is defined via the on-shell one-loop matrix element of the HQET currents

$$\langle\bar{h}_{v'}\,\slashed{n}_+(1\mp\gamma_5)h_v\rangle^{(1)} = \left(Y_{\mathrm{ext}}^{(1)} + Z_{Jh}^{(1)}\right)\langle\bar{h}_{v'}\,\slashed{n}_+(1\mp\gamma_5)h_v\rangle^{(0)}. \qquad (3.7)$$

The one-loop renormalized matrix elements of the QCD currents can be calculated straightforwardly. Inserting their explicit expressions in eq. (3.6) we can identify $Z_{Jh}^{(1)}$ as the pole term in ϵ, that is

$$Z_{Jh}^{(1)} = \frac{C_F}{\epsilon}\left(\frac{(z_c+1)\log(z_c)}{z_c-1} - 2\right), \qquad (3.8)$$

which correctly reproduces the IR behaviour of QCD currents in the effective theory. The C_{FF}, on the other hand, are given by the coefficients that are finite in ϵ. Their explicit expressions read ($L \equiv \log(\mu^2/m_b^2)$)

$$C_{FF}^{\mathrm{D}(1)} = C_F\left[L\left(\frac{(z_c+1)\log(z_c)}{z_c-1} - 2\right) + \frac{(z_c+1)\log^2(z_c)}{2-2z_c} + \frac{(5z_c+1)\log(z_c)}{2(z_c-1)} - 4\right], \quad (3.9)$$
$$C_{FF}^{\mathrm{ND}(1)} = C_F\left(\frac{\sqrt{z_c}\log(z_c)}{z_c-1}\right). \qquad (3.10)$$

As a last step the contribution of the sum $\sum_{b\neq 1} H_{ib}^{(1)}Y_{b1}^{(1)}$ in eq. (2.28) needs to be further specified (the primed quantities are obtained by obvious substitutions). We find

that only $H_{ib}^{(1)}$ with $i = 1$ and $b = 2$ yields a non-vanishing contribution. A straightforward calculation yields $H_{12}^{(1)} = A_{12}^{(1)nf} + Z_{1j}^{(1)} A_{j2}^{(0)}$. The operator renormalization factor $Y_{21}^{(1)}$ has already been used in the NNLO calculation of the vertex corrections to the decay $B \to \pi\pi$ and is given in eq. (45) of [25]. Its explicit expression reads

$$Y_{21}^{(1)}(u', u) = 16\, C_F \left(\frac{u'\Theta(u - u')}{u} + \frac{(1 - u')\Theta(u' - u)}{1 - u} \right) . \qquad (3.11)$$

With this we have specified all input to the master formulas and are now ready to produce an expression for the hard scattering kernels.

The final expressions for the hard scattering kernels are free of poles in ϵ, even though most of the individual terms in eq. (2.28) contain divergences. At the one-loop level we checked the cancellation of all poles analytically. We find that our expressions for the finite pieces of the one-loop kernels agree with the results given in eqs. (89) and (90) in [13].[3] Some of the one-loop quantities that enter the two-loop master formula (last equation in (2.28)) have to be evaluated to higher orders in the ϵ-expansion since they multiply poles in ϵ contained in the renormalization factors. We checked that in the limit $m_c \to 0$ the $\mathcal{O}(\epsilon)$ piece of the one-loop hard scattering kernel coincides with the one used in [28].

At two loops we could check the pole cancellation numerically to an accuracy of 1×10^{-10} or better for 12 different points in the u-z_c plane. To this end, we evaluate the Goncharov polylogarithms and the harmonic polylogarithms [55] that are contained in $A^{(2)nf}$ numerically with the C++ routine GiNaC [56] and the Mathematica program HPL [57, 58], respectively. The explicit results for the two-loop hard scattering kernels are lengthy, not very illuminating, and enter the physical quantities only after convolution with the LCDAs. For these reasons we refrain from presenting them explicitly here, but they can be obtained from the authors upon request. However, after the convolution of the hard scattering kernels with an expansion of the LCDAs in terms of Gegenbauer polynomials up to the second moment, the expressions simplify considerably and we can express the result almost entirely in terms of harmonic polylogarithms. At this level we convolute also the pole terms in ϵ and checked that for the convoluted kernels all poles cancel analytically. We give the corresponding finite parts in the next section.

4 Convoluted kernels

The light meson LCDAs are expanded in a basis of Gegenbauer polynomials $C_k^{3/2}(x)$ with Gegenbauer moments α_k^L,

$$\Phi_L(u, \mu) = 6u(1 - u) \left(1 + \sum_{k=1}^{\infty} \alpha_k^L(\mu) C_k^{3/2}(2u - 1) \right) . \qquad (4.1)$$

Following [13] we assume that the leading-twist LCDA is close to its asymptotic form $\Phi_L(u, \mu) = 6u(1 - u)$ and truncate the expansion after the second moment. The first two

---

[3]For performing this comparison one has to take into account that the one-loop result given in eq. (90) in [13] was calculated in the "traditional operator basis" given in eq. (V.1) in [38].

Gegenbauer polynomials read $C_1^{3/2}(x) = 3x$ and $C_2^{3/2}(x) = \frac{3}{2}(5x^2 - 1)$. The Gegenbauer polynomials are eigenfunctions of the one-loop renormalized ERBL-kernel [59] and thus the Gegenbauer moments are multiplicatively renormalizable to leading-logarithmic (LL) accuracy [59]. The next-to-leading logarithmic (NLL) evolution was derived in [59–61].

The result for the hard scattering kernels after the convolution with the LCDA can be written as follows

$$\int_0^1 du \, \hat{T}_i(u,\mu)\Phi_L(u,\mu) = V_i^{(0)}(\mu) + \sum_{l \geq 1} \left(\frac{\alpha_s}{4\pi}\right)^l \sum_{k=0}^2 \alpha_k^L(\mu) \, V_{ik}^{(l)}(\mu) \,, \tag{4.2}$$

$$\int_0^1 du \, \hat{T}_i'(u,\mu)\Phi_L(u,\mu) = V_i'^{(0)}(\mu) + \sum_{l \geq 1} \left(\frac{\alpha_s}{4\pi}\right)^l \sum_{k=0}^2 \alpha_k^L(\mu) \, V_{ik}'^{(l)}(\mu)\sqrt{z_c} \,, \tag{4.3}$$

with $\alpha_0^L(\mu) \equiv 1$. At tree-level we obtain

$$V_1^{(0)}(\mu) = 0 \,, \quad V_1'^{(0)}(\mu) = 0 \,, \tag{4.4}$$

$$V_2^{(0)}(\mu) = 1 \,, \quad V_2'^{(0)}(\mu) = 0 \,. \tag{4.5}$$

In the following we use the abbreviations $L \equiv \log(\mu^2/m_b^2)$ and $H_{\vec{a}}(z_c) \equiv H_{\vec{a}}$ for the harmonic polylogarithms of argument z_c. The one-loop results for the convoluted colour-octet kernels then read

$$
\begin{aligned}
V_{10}^{(1)}(\mu) = {}&-\frac{4L}{3} + \left[-\frac{4z_c^2}{(z_c-1)^3}H_{00} + \frac{2\left(z_c^2 + 10z_c + 1\right)}{3(z_c-1)^2}H_1 + \frac{2z_c(z_c+1)}{(z_c-1)^2}H_0 \right.\\
&\left. - \frac{4z_c(z_c+1)}{(z_c-1)^3}H_2 + \pi^2\frac{2z_c(z_c+1)}{3(z_c-1)^3} + \frac{-5z_c^2 + 18z_c - 5}{(z_c-1)^2} \right]\\
&+ i\pi\left[-\frac{4z_c^2}{(z_c-1)^3}H_0 + \frac{2(2z_c^2 + 5z_c - 1)}{3(z_c-1)^2} \right],
\end{aligned}
$$

$$
\begin{aligned}
V_{11}^{(1)}(\mu) = {}&\left[-\frac{4z_c^2(z_c+3)}{(z_c-1)^4}H_{00} - \frac{2z_c\left(z_c^2 - 20z_c - 5\right)}{3(z_c-1)^3}H_0 - \frac{4z_c\left(z_c^2 + 6z_c + 1\right)}{(z_c-1)^4}H_2 \right.\\
&- \frac{2\left(z_c^3 - 25z_c^2 - 25z_c + 1\right)}{3(z_c-1)^3}H_1 + \pi^2\frac{2z_c\left(z_c^2 + 6z_c + 1\right)}{3(z_c-1)^4}\\
&\left. + \frac{-11z_c^3 + 155z_c^2 + 155z_c - 11}{9(z_c-1)^3} \right]\\
&+ i\pi\left[-\frac{4z_c^2(z_c+3)}{(z_c-1)^4}H_0 + \frac{-4z_c^3 + 46z_c^2 + 4z_c + 2}{3(z_c-1)^3} \right],
\end{aligned}
$$

$$
\begin{aligned}
V_{12}^{(1)}(\mu) = {}&\left[-\frac{24z_c^2\left(z_c^2 + 3z_c + 1\right)}{(z_c-1)^5}H_{00} + \frac{2(z_c+1)^2\left(z_c^2 + 28z_c + 1\right)}{(z_c-1)^4}H_1 \right.\\
&+ \frac{2z_c\left(z_c^3 + 29z_c^2 + 29z_c + 1\right)}{(z_c-1)^4}H_0 - \frac{24z_c\left(z_c^3 + 4z_c^2 + 4z_c + 1\right)}{(z_c-1)^5}H_2\\
&\left. + \pi^2\frac{4z_c\left(z_c^3 + 4z_c^2 + 4z_c + 1\right)}{(z_c-1)^5} + \frac{-7z_c^4 + 1368z_c^3 + 4478z_c^2 + 1368z_c - 7}{30(z_c-1)^4} \right]\\
&+ i\pi\left[-\frac{24z_c^2\left(z_c^2 + 3z_c + 1\right)}{(z_c-1)^5}H_0 + \frac{2z_c\left(z_c^3 + 29z_c^2 + 29z_c + 1\right)}{(z_c-1)^4} \right],
\end{aligned}
$$

$$
V_{10}^{\prime(1)}(\mu) = \left[\frac{4z_c(z_c + 2)}{3(z_c - 1)^3} H_{00} + \frac{4\left(z_c^2 + 4z_c + 1\right)}{3(z_c - 1)^3} H_2 - \frac{2(5z_c + 1)}{3(z_c - 1)^2} H_0 - \frac{4(z_c + 1)}{(z_c - 1)^2} H_1 \right.
$$
$$
\left. - \pi^2 \frac{2\left(z_c^2 + 4z_c + 1\right)}{9(z_c - 1)^3} - \frac{4(z_c + 1)}{(z_c - 1)^2} \right] + i\pi \left[\frac{4z_c(z_c + 2)}{3(z_c - 1)^3} H_0 - \frac{2(5z_c + 1)}{3(z_c - 1)^2} \right],
$$
$$
V_{11}^{\prime(1)}(\mu) = \left[-\frac{4z_c\left(z_c^2 + 5z_c + 2\right)}{(z_c - 1)^4} H_{00} + \frac{2\left(19z_c^2 + 28z_c + 1\right)}{3(z_c - 1)^3} H_0 \right.
$$
$$
+ \frac{8\left(5z_c^2 + 14z_c + 5\right)}{3(z_c - 1)^3} H_1 - \frac{4\left(z_c^3 + 7z_c^2 + 7z_c + 1\right)}{(z_c - 1)^4} H_2
$$
$$
\left. + \pi^2 \frac{2\left(z_c^3 + 7z_c^2 + 7z_c + 1\right)}{3(z_c - 1)^4} + \frac{2\left(41z_c^2 + 206z_c + 41\right)}{9(z_c - 1)^3} \right]
$$
$$
+ i\pi \left[-\frac{4z_c\left(z_c^2 + 5z_c + 2\right)}{(z_c - 1)^4} H_0 + \frac{2\left(19z_c^2 + 28z_c + 1\right)}{3(z_c - 1)^3} \right],
$$
$$
V_{12}^{\prime(1)}(\mu) = \left[\frac{8z_c\left(z_c^3 + 10z_c^2 + 12z_c + 2\right)}{(z_c - 1)^5} H_{00} - \frac{2\left(45z_c^3 + 181z_c^2 + 73z_c + 1\right)}{3(z_c - 1)^4} H_0 \right.
$$
$$
- \frac{4\left(23z_c^3 + 127z_c^2 + 127z_c + 23\right)}{3(z_c - 1)^4} H_1 + \frac{8\left(z_c^4 + 12z_c^3 + 24z_c^2 + 12z_c + 1\right)}{(z_c - 1)^5} H_2
$$
$$
\left. - \pi^2 \frac{4\left(z_c^4 + 12z_c^3 + 24z_c^2 + 12z_c + 1\right)}{3(z_c - 1)^5} - \frac{2\left(73z_c^3 + 827z_c^2 + 827z_c + 73\right)}{9(z_c - 1)^4} \right]
$$
$$
+ i\pi \left[\frac{8z_c\left(z_c^3 + 10z_c^2 + 12z_c + 2\right)}{(z_c - 1)^5} H_0 - \frac{2\left(45z_c^3 + 181z_c^2 + 73z_c + 1\right)}{3(z_c - 1)^4} \right]. \quad (4.6)
$$

The one-loop colour-singlet kernels vanish as the corresponding colour factors are zero,

$$
V_{2k}^{(1)}(\mu) = V_{2k}^{\prime(1)}(\mu) = 0, \quad \text{for} \quad k = 0, 1, 2. \quad (4.7)
$$

At two loops the result is rather lengthy. Here, we only present the full result for the μ-dependent part which governs the scale dependence. For the μ-independent part we provide a fitted function in z_c that agrees with the original result at the per mill level in the range of physical values $0.05 \leq z_c \leq 0.2$. The full result is attached in electronic form to the arXiv submission of the present work. For the convoluted colour-octet kernels we obtain

$$
V_{10}^{(2)}(\mu) = -\frac{58}{9} L^2 + \left[-\frac{116z_c^2}{3(z_c - 1)^3} H_{00} + \frac{58\left(z_c^2 + 10z_c + 1\right)}{9(z_c - 1)^2} H_1 + \frac{58z_c(z_c + 1)}{3(z_c - 1)^2} H_0 \right.
$$
$$
\left. - \frac{116z_c(z_c + 1)}{3(z_c - 1)^3} H_2 + \pi^2 \frac{58z_c(z_c + 1)}{9(z_c - 1)^3} - \frac{2\left(527z_c^2 - 2098z_c + 527\right)}{27(z_c - 1)^2} \right] L
$$
$$
+ i\pi \left[-\frac{116z_c^2}{3(z_c - 1)^3} H_0 + \frac{58\left(2z_c^2 + 5z_c - 1\right)}{9(z_c - 1)^2} \right] L
$$
$$
+ \left[66.8297 z_c^2 - 43.9087 z_c - 75.8620 - \frac{0.148459}{z_c} - 9.68071 \log(z_c) \right]
$$
$$
+ i\pi \left[-14.7418 z_c^2 + 37.9194 z_c - 23.9326 + \frac{0.0130025}{z_c} + 0.263367 \log(z_c) \right],
$$

$$V_{11}^{(2)}(\mu) = \left[-\frac{476 z_c^2 (z_c + 3)}{9(z_c - 1)^4} H_{00} - \frac{238 z_c \left(z_c^2 - 20 z_c - 5\right)}{27(z_c - 1)^3} H_0 - \frac{476 z_c \left(z_c^2 + 6 z_c + 1\right)}{9(z_c - 1)^4} H_2 \right.$$

$$- \frac{238 \left(z_c^3 - 25 z_c^2 - 25 z_c + 1\right)}{27(z_c - 1)^3} H_1 + \pi^2 \frac{238 z_c \left(z_c^2 + 6 z_c + 1\right)}{27(z_c - 1)^4}$$

$$\left. - \frac{119 \left(11 z_c^3 - 155 z_c^2 - 155 z_c + 11\right)}{81(z_c - 1)^3} \right] L$$

$$+ i\pi \left[-\frac{476(z_c + 3) z_c^2}{9(z_c - 1)^4} H_0 - \frac{238 \left(2 z_c^3 - 23 z_c^2 - 2 z_c - 1\right)}{27(z_c - 1)^3} \right] L$$

$$+ \left[-86.0751 z_c^2 + 71.1970 z_c + 228.207 + \frac{0.273411}{z_c} + 20.6412 \log(z_c) \right]$$

$$+ i\pi \left[-105.333 z_c - 18.1118 - \frac{0.0625952}{z_c} - 3.09381 \log(z_c) \right],$$

$$V_{12}^{(2)}(\mu) = \left[-\frac{1096 z_c^2 \left(z_c^2 + 3 z_c + 1\right)}{3(z_c - 1)^5} H_{00} + \frac{274(z_c + 1)^2 \left(z_c^2 + 28 z_c + 1\right)}{9(z_c - 1)^4} H_1 \right.$$

$$+ \frac{274 z_c \left(z_c^3 + 29 z_c^2 + 29 z_c + 1\right)}{9(z_c - 1)^4} H_0 - \frac{1096 z_c \left(z_c^3 + 4 z_c^2 + 4 z_c + 1\right)}{3(z_c - 1)^5} H_2$$

$$+ \pi^2 \frac{548 z_c \left(z_c^3 + 4 z_c^2 + 4 z_c + 1\right)}{9(z_c - 1)^5}$$

$$\left. - \frac{137 \left(7 z_c^4 - 1368 z_c^3 - 4478 z_c^2 - 1368 z_c + 7\right)}{270(z_c - 1)^4} \right] L$$

$$+ i\pi \left[-\frac{1096 z_c^2 \left(z_c^2 + 3 z_c + 1\right)}{3(z_c - 1)^5} H_0 + \frac{274 z_c \left(z_c^3 + 29 z_c^2 + 29 z_c + 1\right)}{9(z_c - 1)^4} \right] L$$

$$+ \left[-125.04 z_c^2 + 86.9295 z_c - 26.8151 + \frac{0.11072}{z_c} + 0.595046 \log(z_c) \right]$$

$$+ i\pi \left[-20.971087 z_c^3 + 49.652981 z_c^2 - 65.251113 z_c + 32.324740 - \frac{0.054806548}{z_c} \right.$$

$$\left. + \frac{0.000082559030}{z_c^2} + 15.519430 \log(z_c) + 1.9371679 \log^2(z_c) \right],$$

$$V_{10}^{\prime(2)}(\mu) = \left[\frac{116 z_c(z_c + 2)}{9(z_c - 1)^3} H_{00} + \frac{116 \left(z_c^2 + 4 z_c + 1\right)}{9(z_c - 1)^3} H_2 - \frac{58(5 z_c + 1)}{9(z_c - 1)^2} H_0 \right.$$

$$\left. - \frac{116(z_c + 1)}{3(z_c - 1)^2} H_1 - \pi^2 \frac{58 \left(z_c^2 + 4 z_c + 1\right)}{27(z_c - 1)^3} - \frac{116(z_c + 1)}{3(z_c - 1)^2} \right] L$$

$$+ i\pi \left[\frac{116 z_c(z_c + 2)}{9(z_c - 1)^3} H_0 - \frac{58(5 z_c + 1)}{9(z_c - 1)^2} \right] L$$

$$+ \left[32.231179 z_c^3 - 58.177605 z_c^2 + 81.440153 z_c - 76.877229 - \frac{0.16778620}{z_c} \right.$$

$$\left. + \frac{0.00063267263}{z_c^2} - 33.071605 \log(z_c) + 0.97638808 \log^2(z_c) \right]$$

$$+ i\pi \left[-30.6744 z_c^2 + 35.2510 z_c - 17.1594 + \frac{0.0920248}{z_c} + 1.56243 \log(z_c) \right],$$

$$
\begin{aligned}
V_{11}^{\prime(2)}(\mu) = \Bigg[& -\frac{476 z_c \left(z_c^2 + 5 z_c + 2\right)}{9(z_c - 1)^4} H_{00} + \frac{238 \left(19 z_c^2 + 28 z_c + 1\right)}{27(z_c - 1)^3} H_0 \\
& + \frac{952 \left(5 z_c^2 + 14 z_c + 5\right)}{27(z_c - 1)^3} H_1 - \frac{476 \left(z_c^3 + 7 z_c^2 + 7 z_c + 1\right)}{9(z_c - 1)^4} H_2 \\
& + \pi^2 \frac{238 \left(z_c^3 + 7 z_c^2 + 7 z_c + 1\right)}{27(z_c - 1)^4} + \frac{238 \left(41 z_c^2 + 206 z_c + 41\right)}{81(z_c - 1)^3} \Bigg] L \\
& + i\pi \Bigg[-\frac{476 z_c \left(z_c^2 + 5 z_c + 2\right)}{9(z_c - 1)^4} H_0 + \frac{238 \left(19 z_c^2 + 28 z_c + 1\right)}{27(z_c - 1)^3} \Bigg] L \\
& + \Bigg[-234.47 z_c^2 + 316.827 z_c - 148.270 + \frac{1.51374}{z_c} - \frac{0.0135728}{z_c^2} - 32.2242 \log(z_c) \Bigg] \\
& + i\pi \Bigg[-3.48636 z_c^2 - 33.7104 z_c + 37.2121 + \frac{0.702284}{z_c} \\
& \quad - \frac{0.00455572}{z_c^2} + 22.4084 \log(z_c) \Bigg],
\end{aligned}
$$

$$
\begin{aligned}
V_{12}^{\prime(2)}(\mu) = \Bigg[& \frac{1096 z_c \left(z_c^3 + 10 z_c^2 + 12 z_c + 2\right)}{9(z_c - 1)^5} H_{00} - \frac{274 \left(45 z_c^3 + 181 z_c^2 + 73 z_c + 1\right)}{27(z_c - 1)^4} H_0 \\
& - \frac{548 \left(23 z_c^3 + 127 z_c^2 + 127 z_c + 23\right)}{27(z_c - 1)^4} H_1 + \frac{1096 \left(z_c^4 + 12 z_c^3 + 24 z_c^2 + 12 z_c + 1\right)}{9(z_c - 1)^5} H_2 \\
& - \pi^2 \frac{548 \left(z_c^4 + 12 z_c^3 + 24 z_c^2 + 12 z_c + 1\right)}{27(z_c - 1)^5} - \frac{274 \left(73 z_c^3 + 827 z_c^2 + 827 z_c + 73\right)}{81(z_c - 1)^4} \Bigg] L \\
& + i\pi \Bigg[\frac{1096 z_c \left(z_c^3 + 10 z_c^2 + 12 z_c + 2\right)}{9(z_c - 1)^5} H_0 - \frac{274 \left(45 z_c^3 + 181 z_c^2 + 73 z_c + 1\right)}{27(z_c - 1)^4} \Bigg] L \\
& + \Bigg[-213.310 z_c^2 + 115.262 z_c + 3.64826 + \frac{4.51494}{z_c} \\
& \quad - \frac{0.0350821}{z_c^2} + 37.7768 \log(z_c) \Bigg] \\
& + i\pi \Bigg[-120.66419 z_c^3 + 202.98069 z_c^2 - 192.44717 z_c \\
& \quad + 84.350652 + \frac{0.59574628}{z_c} - \frac{0.0025637896}{z_c^2} + 34.327758 \log(z_c) \Bigg].
\end{aligned} \tag{4.8}
$$

The result for the convoluted colour-singlet kernels takes the form

$$
\begin{aligned}
V_{20}^{(2)}(\mu) = 4 L^2 + \Bigg[& \frac{24 z_c^2}{(z_c - 1)^3} H_{00} - \frac{4 \left(z_c^2 + 10 z_c + 1\right)}{(z_c - 1)^2} H_1 - \frac{12 z_c (z_c + 1)}{(z_c - 1)^2} H_0 \\
& + \frac{24 z_c (z_c + 1)}{(z_c - 1)^3} H_2 - \pi^2 \frac{4 z_c (z_c + 1)}{(z_c - 1)^3} + \frac{8 \left(13 z_c^2 - 44 z_c + 13\right)}{3(z_c - 1)^2} \Bigg] L \\
& + i\pi \Bigg[\frac{24 z_c^2}{(z_c - 1)^3} H_0 - \frac{4 \left(2 z_c^2 + 5 z_c - 1\right)}{(z_c - 1)^2} \Bigg] L \\
& + \Bigg[55.3728 z_c + 92.1737 + \frac{0.107621}{z_c} + 5.69272 \log(z_c) \Bigg] \\
& + i\pi \Bigg[-8.26434 z_c + 23.3800 - \frac{0.0109724}{z_c} - 0.0317131 \log(z_c) \Bigg],
\end{aligned}
$$

$$V_{21}^{(2)}(\mu) = \left[\frac{24z_c^2(z_c+3)}{(z_c-1)^4} H_{00} + \frac{4z_c\left(z_c^2-20z_c-5\right)}{(z_c-1)^3} H_0 + \frac{24z_c\left(z_c^2+6z_c+1\right)}{(z_c-1)^4} H_2 \right.$$

$$+ \frac{4\left(z_c^3-25z_c^2-25z_c+1\right)}{(z_c-1)^3} H_1 - \pi^2 \frac{4z_c\left(z_c^2+6z_c+1\right)}{(z_c-1)^4}$$

$$\left. + \frac{2\left(11z_c^3-155z_c^2-155z_c+11\right)}{3(z_c-1)^3} \right] L$$

$$+ i\pi \left[\frac{24(z_c+3)z_c^2}{(z_c-1)^4} H_0 + \frac{8z_c^3-92z_c^2-8z_c-4}{(z_c-1)^3} \right] L$$

$$+ \left[113.426z_c - 94.6182 - \frac{0.188354}{z_c} - 12.3877\log(z_c) \right]$$

$$+ i\pi \left[-53.5714z_c^2 + 48.8676z_c + 16.8809 + \frac{0.0506772}{z_c} + 2.03180\log(z_c) \right],$$

$$V_{22}^{(2)}(\mu) = \left[\frac{144z_c^2\left(z_c^2+3z_c+1\right)}{(z_c-1)^5} H_{00} - \frac{12(z_c+1)^2\left(z_c^2+28z_c+1\right)}{(z_c-1)^4} H_1 \right.$$

$$- \frac{12z_c\left(z_c^3+29z_c^2+29z_c+1\right)}{(z_c-1)^4} H_0 + \frac{144z_c\left(z_c^3+4z_c^2+4z_c+1\right)}{(z_c-1)^5} H_2$$

$$\left. - \pi^2 \frac{24z_c\left(z_c^3+4z_c^2+4z_c+1\right)}{(z_c-1)^5} + \frac{7z_c^4-1368z_c^3-4478z_c^2-1368z_c+7}{5(z_c-1)^4} \right] L$$

$$+ i\pi \left[\frac{144z_c^2\left(z_c^2+3z_c+1\right)}{(z_c-1)^5} H_0 - \frac{12z_c\left(z_c^3+29z_c^2+29z_c+1\right)}{(z_c-1)^4} \right] L$$

$$+ \left[-170.55583z_c^3 + 246.55778z_c^2 - 183.90296z_c + 23.796978 \right.$$

$$\left. + \frac{0.024080798}{z_c} + \frac{0.00019457018}{z_c^2} + 4.9343948\log(z_c) \right]$$

$$+ i\pi \left[23.5064z_c - 21.2951 - \frac{0.219828}{z_c} + \frac{0.00168271}{z_c^2} - 6.22465\log(z_c) \right],$$

$$V_{20}'^{(2)}(\mu) = \left[-\frac{8z_c(z_c+2)}{(z_c-1)^3} H_{00} - \frac{8\left(z_c^2+4z_c+1\right)}{(z_c-1)^3} H_2 + \frac{4(5z_c+1)}{(z_c-1)^2} H_0 + \frac{24(z_c+1)}{(z_c-1)^2} H_1 \right.$$

$$\left. + \pi^2 \frac{4\left(z_c^2+4z_c+1\right)}{3(z_c-1)^3} + \frac{24(z_c+1)}{(z_c-1)^2} \right] L + i\pi \left[\frac{4(5z_c+1)}{(z_c-1)^2} - \frac{8z_c(z_c+2)}{(z_c-1)^3} H_0 \right] L$$

$$+ \left[11.757344z_c^2 + 2.3337593z_c - 14.515538 + \frac{0.55463304}{z_c} \right.$$

$$\left. - \frac{0.0021489969}{z_c^2} - 19.152880\log(z_c) - 6.9182541\log^2(z_c) \right]$$

$$+ i\pi \left[9.07488z_c - 8.30981 - \frac{0.203702}{z_c} + \frac{0.00146545}{z_c^2} - 5.78268\log(z_c) \right],$$

$$V_{21}'^{(2)}(\mu) = \left[\frac{24z_c\left(z_c^2+5z_c+2\right)}{(z_c-1)^4} H_{00} - \frac{4\left(19z_c^2+28z_c+1\right)}{(z_c-1)^3} H_0 - \frac{16\left(5z_c^2+14z_c+5\right)}{(z_c-1)^3} H_1 \right.$$

$$+ \frac{24\left(z_c^3+7z_c^2+7z_c+1\right)}{(z_c-1)^4} H_2 - \pi^2 \frac{4\left(z_c^3+7z_c^2+7z_c+1\right)}{(z_c-1)^4}$$

$$\left. - \frac{4\left(41z_c^2+206z_c+41\right)}{3(z_c-1)^3} \right] L$$

$$
\begin{aligned}
&+ i\pi \left[\frac{24z_c \left(z_c^2 + 5z_c + 2\right)}{(z_c - 1)^4} H_0 - \frac{4\left(19z_c^2 + 28z_c + 1\right)}{(z_c - 1)^3} \right] L \\
&+ \left[-547.207z_c^3 + 426.128z_c^2 - 113.484z_c + 0.744742 - \frac{0.212278}{z_c} \right] \\
&+ i\pi \left[-80.143647z_c^4 + 141.27932z_c^3 - 118.74488z_c^2 + 64.799529z_c \right. \\
&\qquad \left. - 16.163881 - \frac{0.045527818}{z_c} - 4.6034803\log(z_c) \right], \\
V_{22}^{\prime(2)}(\mu) = &\left[-\frac{48z_c \left(z_c^3 + 10z_c^2 + 12z_c + 2\right)}{(z_c - 1)^5} H_{00} + \frac{4\left(45z_c^3 + 181z_c^2 + 73z_c + 1\right)}{(z_c - 1)^4} H_0 \right. \\
&+ \frac{8\left(23z_c^3 + 127z_c^2 + 127z_c + 23\right)}{(z_c - 1)^4} H_1 - \frac{48\left(z_c^4 + 12z_c^3 + 24z_c^2 + 12z_c + 1\right)}{(z_c - 1)^5} H_2 \\
&+ \pi^2 \frac{8\left(z_c^4 + 12z_c^3 + 24z_c^2 + 12z_c + 1\right)}{(z_c - 1)^5} + \left. \frac{4\left(73z_c^3 + 827z_c^2 + 827z_c + 73\right)}{3(z_c - 1)^4} \right] L \\
&+ i\pi \left[\frac{4\left(45z_c^3 + 181z_c^2 + 73z_c + 1\right)}{(z_c - 1)^4} - \frac{48z_c \left(z_c^3 + 10z_c^2 + 12z_c + 2\right)}{(z_c - 1)^5} H_0 \right] L \\
&+ \left[-122.195z_c^2 + 118.502z_c - 37.1904 - \frac{0.0663899}{z_c} \right. \\
&\qquad \left. - \frac{0.00227343}{z_c^2} - 9.22903\log(z_c) \right] \\
&+ i\pi \left[-170.35896z_c^4 + 201.55736z_c^3 - 93.946885z_c^2 + 7.9715007z_c \right. \\
&\qquad + 7.3620315 + \frac{0.34672826}{z_c} - \frac{0.0045037110}{z_c^2} + \frac{0.000031922024}{z_c^3} \\
&\qquad \left. + 4.4579847\log(z_c) \right]. \tag{4.9}
\end{aligned}
$$

Finally, we checked with the full result (without interpolation in z_c) that in the limit $m_c \to 0$ eq. (4.2) with $\mu = m_b$ coincides with the result for the vertex corrections to the colour-allowed tree topology of the decay $B \to \pi\pi$ given in eq. (48) of [28].

5 Conversion from the pole to the $\overline{\text{MS}}$ scheme

The convoluted kernels in eqs. (4.2) and (4.3) are given in the pole scheme, where m_c and m_b appearing in $L \equiv \log(\mu^2/m_b^2)$ and $z_c = m_c^2/m_b^2$ denote the pole quark masses, and the renormalization scale $\mu \sim m_b$. In order to discuss the scheme dependence of the convoluted kernels, we also give the results in the $\overline{\text{MS}}$ scheme for the quark masses. Since the LO kernels are constant and the NLO colour-singlet kernels vanish, the conversion from the pole to the $\overline{\text{MS}}$ scheme will only affect the NNLO colour-octet kernels $V_{1k}^{(2)}$ and $V_{1k}^{\prime(2)}$. To this end, using the one-loop relation between pole- and $\overline{\text{MS}}$-quark mass,

$$
m_q = \overline{m}_q(\mu) \left[1 + \frac{\alpha_s}{\pi} \left(\frac{4}{3} + \log\left(\frac{\mu^2}{\overline{m}_q^2(\mu)} \right) \right) \right], \tag{5.1}
$$

we find that the corresponding convoluted kernels in the $\overline{\text{MS}}$ scheme are obtained via the relation

$$V_{1k}^{(\prime)\overline{\text{MS}}(2)}(\mu) = V_{1k}^{(\prime)(2)} + \Delta V_{1k}^{(\prime)},$$

$$\Delta V_{1k} = -8z_c \ln(z_c)\frac{\partial V_{1k}^{(1)}}{\partial z_c} - \left[\frac{32}{3} + 8L\right]\frac{\partial V_{1k}^{(1)}}{\partial L},$$

$$\Delta V_{1k}' = -8\sqrt{z_c}\ln(z_c)\frac{\partial\sqrt{z_c}V_{1k}'^{(1)}}{\partial z_c} - \left[\frac{32}{3} + 8L\right]\frac{\partial V_{1k}'^{(1)}}{\partial L}, \qquad (5.2)$$

where now $L \equiv \log(\mu^2/\overline{m}_b^2(\mu))$ and $z_c = \overline{m}_c^2(\mu)/\overline{m}_b^2(\mu)$, with $\mu \sim \overline{m}_b(\overline{m}_b)$.

The tree-level and one-loop kernels will have the same functional dependence as in the pole scheme, but now depend on the above new abbreviations in the $\overline{\text{MS}}$ scheme. At two loops we explicitly give the terms that have to be added,

$$\Delta V_{10} = \frac{32}{3}L + \left[-\frac{32z_c\left(z_c^2 + 4z_c + 1\right)}{(z_c - 1)^4}H_{20} - \frac{96z_c^2(z_c + 2)}{(z_c - 1)^4}H_{000} + \frac{32z_c(5z_c + 1)}{(z_c - 1)^3}H_{00} \right.$$

$$+ \frac{96z_c(z_c + 1)}{(z_c - 1)^3}H_{10} - \frac{32z_c\left(z_c^2 - 11z_c - 8\right)}{3(z_c - 1)^3}H_0 - \frac{64z_c\left(z_c^2 + 4z_c + 1\right)}{(z_c - 1)^4}H_3$$

$$\left. + \frac{96z_c(z_c + 1)}{(z_c - 1)^3}H_2 + \pi^2\frac{16z_c\left(z_c^2 + 4z_c + 1\right)}{3(z_c - 1)^4}H_0 + \frac{128}{9}\right]$$

$$+ i\pi\left[\frac{16z_c(5z_c + 1)}{(z_c - 1)^3}H_0 - \frac{64z_c^2(z_c + 2)}{(z_c - 1)^4}H_{00}\right],$$

$$\Delta V_{11} = \left[\frac{32z_c\left(23z_c^2 + 68z_c + 5\right)}{3(z_c - 1)^4}H_{00} + \frac{64z_c\left(7z_c^2 + 34z_c + 7\right)}{3(z_c - 1)^4}H_{10}\right.$$

$$- \frac{96z_c^2\left(z_c^2 + 9z_c + 6\right)}{(z_c - 1)^5}H_{000} - \frac{32z_c\left(z_c^3 + 15z_c^2 + 15z_c + 1\right)}{(z_c - 1)^5}H_{20}$$

$$+ \frac{16z_c\left(73z_c^2 + 430z_c + 73\right)}{9(z_c - 1)^4}H_0 + \frac{64z_c\left(7z_c^2 + 34z_c + 7\right)}{3(z_c - 1)^4}H_2$$

$$\left. - \frac{64z_c\left(z_c^3 + 15z_c^2 + 15z_c + 1\right)}{(z_c - 1)^5}H_3 + \pi^2\frac{16z_c\left(z_c^3 + 15z_c^2 + 15z_c + 1\right)}{3(z_c - 1)^5}H_0\right]$$

$$+ i\pi\left[\frac{16H_0z_c\left(23z_c^2 + 68z_c + 5\right)}{3(z_c - 1)^4} - \frac{64z_c^2\left(z_c^2 + 9z_c + 6\right)H_{00}}{(z_c - 1)^5}\right],$$

$$\Delta V_{12} = \left[\frac{32z_c\left(45z_c^3 + 181z_c^2 + 73z_c + 1\right)}{(z_c - 1)^5}H_{00} + \frac{32z_c\left(23z_c^3 + 127z_c^2 + 127z_c + 23\right)}{(z_c - 1)^5}H_{10}\right.$$

$$- \frac{576z_c^2\left(z_c^3 + 10z_c^2 + 12z_c + 2\right)}{(z_c - 1)^6}H_{000} + \frac{32z_c\left(23z_c^3 + 127z_c^2 + 127z_c + 23\right)}{(z_c - 1)^5}H_2$$

$$- \frac{192z_c\left(z_c^4 + 12z_c^3 + 24z_c^2 + 12z_c + 1\right)}{(z_c - 1)^6}H_{20}$$

$$- \frac{384z_c\left(z_c^4 + 12z_c^3 + 24z_c^2 + 12z_c + 1\right)}{(z_c - 1)^6}H_3$$

$$+ \frac{16z_c\left(73z_c^3 + 827z_c^2 + 827z_c + 73\right)}{3(z_c - 1)^5}H_0$$

$$
\left. + \pi^2 \frac{32 z_c \left(z_c^4 + 12 z_c^3 + 24 z_c^2 + 12 z_c + 1\right) H_0}{(z_c - 1)^6} \right] \tag{5.3}
$$

$$
+ i\pi \left[\frac{16 z_c \left(45 z_c^3 + 181 z_c^2 + 73 z_c + 1\right)}{(z_c - 1)^5} H_0 - \frac{384 z_c^2 \left(z_c^3 + 10 z_c^2 + 12 z_c + 2\right)}{(z_c - 1)^6} H_{00} \right],
$$

$$
\Delta V_{10}' = \left[-\frac{16 \left(9 z_c^2 + 26 z_c + 1\right)}{3(z_c - 1)^3} H_{00} - \frac{16 \left(5 z_c^2 + 26 z_c + 5\right)}{3(z_c - 1)^3} H_{10} - \frac{64 H_0 \left(z_c^2 + 7 z_c + 1\right)}{3(z_c - 1)^3} \right.
$$

$$
+ \frac{16 z_c \left(z_c^2 + 11 z_c + 6\right)}{(z_c - 1)^4} H_{000} + \frac{16 \left(z_c^3 + 17 z_c^2 + 17 z_c + 1\right)}{3(z_c - 1)^4} H_{20}
$$

$$
- \frac{16 \left(5 z_c^2 + 26 z_c + 5\right)}{3(z_c - 1)^3} H_2 + \frac{32 \left(z_c^3 + 17 z_c^2 + 17 z_c + 1\right)}{3(z_c - 1)^4} H_3
$$

$$
\left. - \pi^2 \frac{8 \left(z_c^3 + 17 z_c^2 + 17 z_c + 1\right)}{9(z_c - 1)^4} H_0 \right]
$$

$$
+ i\pi \left[\frac{32 z_c \left(z_c^2 + 11 z_c + 6\right)}{3(z_c - 1)^4} H_{00} - \frac{8 \left(9 z_c^2 + 26 z_c + 1\right)}{3(z_c - 1)^3} H_0 \right],
$$

$$
\Delta V_{11}' = \left[\frac{16 \left(31 z_c^3 + 239 z_c^2 + 113 z_c + 1\right)}{3(z_c - 1)^4} H_{00} + \frac{256 \left(z_c^3 + 11 z_c^2 + 11 z_c + 1\right)}{3(z_c - 1)^4} H_{10} \right.
$$

$$
- \frac{48 z_c \left(z_c^3 + 22 z_c^2 + 35 z_c + 6\right)}{(z_c - 1)^5} H_{000} - \frac{16 \left(z_c^4 + 28 z_c^3 + 70 z_c^2 + 28 z_c + 1\right)}{(z_c - 1)^5} H_{20}
$$

$$
+ \frac{8 \left(47 z_c^3 + 1105 z_c^2 + 1105 z_c + 47\right)}{9(z_c - 1)^4} H_0 + \frac{256 \left(z_c^3 + 11 z_c^2 + 11 z_c + 1\right)}{3(z_c - 1)^4} H_2
$$

$$
\left. - \frac{32 \left(z_c^4 + 28 z_c^3 + 70 z_c^2 + 28 z_c + 1\right)}{(z_c - 1)^5} H_3 + \pi^2 \frac{8 \left(z_c^4 + 28 z_c^3 + 70 z_c^2 + 28 z_c + 1\right)}{3(z_c - 1)^5} H_0 \right]
$$

$$
+ i\pi \left[\frac{8 \left(31 z_c^3 + 239 z_c^2 + 113 z_c + 1\right)}{3(z_c - 1)^4} H_0 - \frac{32 z_c \left(z_c^3 + 22 z_c^2 + 35 z_c + 6\right)}{(z_c - 1)^5} H_{00} \right],
$$

$$
\Delta V_{12}' = \left[-\frac{16 \left(69 z_c^4 + 1098 z_c^3 + 1558 z_c^2 + 274 z_c + 1\right)}{3(z_c - 1)^5} H_{00} \right.
$$

$$
- \frac{16 \left(35 z_c^4 + 686 z_c^3 + 1558 z_c^2 + 686 z_c + 35\right)}{3(z_c - 1)^5} H_{10}
$$

$$
+ \frac{96 z_c \left(z_c^4 + 39 z_c^3 + 130 z_c^2 + 74 z_c + 6\right)}{(z_c - 1)^6} H_{000}
$$

$$
+ \frac{32 \left(z_c^5 + 45 z_c^4 + 204 z_c^3 + 204 z_c^2 + 45 z_c + 1\right)}{(z_c - 1)^6} H_{20}
$$

$$
- \frac{8 \left(79 z_c^4 + 3700 z_c^3 + 10442 z_c^2 + 3700 z_c + 79\right)}{9(z_c - 1)^5} H_0
$$

$$
- \frac{16 \left(35 z_c^4 + 686 z_c^3 + 1558 z_c^2 + 686 z_c + 35\right)}{3(z_c - 1)^5} H_2
$$

$$
+ \frac{64 \left(z_c^5 + 45 z_c^4 + 204 z_c^3 + 204 z_c^2 + 45 z_c + 1\right)}{(z_c - 1)^6} H_3
$$

$$
\left. - \pi^2 \frac{16 \left(z_c^5 + 45 z_c^4 + 204 z_c^3 + 204 z_c^2 + 45 z_c + 1\right)}{3(z_c - 1)^6} H_0 \right]
$$

$$+ i\pi \left[\frac{64 z_c \left(z_c^4 + 39 z_c^3 + 130 z_c^2 + 74 z_c + 6 \right)}{(z_c - 1)^6} H_{00} \right.$$
$$\left. - \frac{8 \left(69 z_c^4 + 1098 z_c^3 + 1558 z_c^2 + 274 z_c + 1 \right)}{3 (z_c - 1)^5} H_0 \right]. \tag{5.4}$$

6 Phenomenological applications

In this section we perform an extensive phenomenological analysis of $\bar{B}_{(s)} \to D_{(s)}^{(*)+} L^-$ and $\Lambda_b \to \Lambda_c^+ L^-$ decays in QCDF. Like before, L is a light meson from the set $\{\pi, \rho, K^{(*)}, a_1\}$. We take into account the expressions through to NNLO for the hard scattering kernels, and the most recent values for non-perturbative input parameters, which we specify below. We analyze the impact of the NNLO correction on the topological tree amplitude $a_1(D^{(*)+} L^-)$, and subsequently predict the branching ratios for the mesonic decays. Afterwards, we perform tests of QCD factorization by considering suitably chosen ratios of non-leptonic to either semi-leptonic or non-leptonic channels. Finally, we give the theoretical predictions for baryonic decays.

6.1 Input parameters

Here we collect in table 1 the theoretical input parameters entering our numerical analysis throughout this paper. They include the SM parameters such as the CKM matrix elements, quark masses, and the strong coupling constant, as well as the hadronic parameters such as meson decay constants, transition form factors, and the Gegenbauer moments of light mesons. Three-loop running is used for α_s throughout this paper. Furthermore, we use a two-loop relation between pole and $\overline{\text{MS}}$ mass to convert the top-quark pole mass m_t^{pole} to the scale-invariant mass $\overline{m}_t(\overline{m}_t)$ [75].

For the $B \to D^{(*)}$ transition form factors, we adopt the parameterization proposed by Caprini, Lellouch, and Neubert (CLN) [76], with the relevant parameters extracted from exclusive semileptonic $b \to c \ell \nu_\ell$ decays [66]. For the $B_s \to D_s^{(*)}$ transition form factors, on the other hand, we use the results obtained by QCD sum-rule techniques, assuming a polar dependence on q^2 that is dominated by the nearest resonance [69, 77]. However, to discuss the SU(3)-breaking effects in the form-factor and decay-constant ratios, we adopt the most recent lattice QCD results for the ratios [70, 78]

$$\frac{F_0^{B_s \to D_s}(m_\pi^2)}{F_0^{B \to D}(m_\pi^2)} = 1.054 \pm 0.047_{\text{stat.}} \pm 0.017_{\text{syst.}},$$
$$\frac{F_0^{B_s \to D_s}(m_\pi^2)}{F_0^{B \to D}(m_K^2)} = 1.046 \pm 0.044_{\text{stat.}} \pm 0.015_{\text{syst.}},$$
$$\frac{f_K}{f_\pi} = 1.1927 \pm 0.0026. \tag{6.1}$$

Neither of the form-factor ratios shows significant deviation from the U-spin symmetry.

For the $\Lambda_b \to \Lambda_c$ transition form factors, we use the most recent high-precision lattice QCD calculation with $2 + 1$ dynamical flavours [36]. Here the q^2 dependence of the form

QCD and electroweak parameters						
	$G_F[10^{-5}\text{GeV}^{-2}]$	$\alpha_s(m_Z)$	$m_Z[\text{GeV}]$	$m_W[\text{GeV}]$		[62]
	1.1663787	0.1185 ± 0.0006	91.1876	80.385		

Quark masses [GeV]						
m_t^{pole}	m_b^{pole}	m_c^{pole}	$\overline{m}_t(\overline{m}_t)$	$\overline{m}_b(\overline{m}_b)$	$\overline{m}_c(\overline{m}_c)$	[62, 63]
173.34 ± 0.76	4.78 ± 0.06	1.67 ± 0.07	163.99 ± 0.72	4.18 ± 0.03	1.275 ± 0.025	

CKM matrix elements				
	$|V_{ud}|$	$|V_{us}|$	$|V_{cb}|_{\text{exclusive}}[10^{-3}]$	[62, 64, 65]
	0.97417 ± 0.00021	0.2253 ± 0.0008	39.5 ± 0.8	

Lifetimes and masses of $B_{d,s}$ and Λ_b						
$\tau_{B_d}[\text{ps}]$	$\tau_{B_s}[\text{ps}]$	$\tau_{\Lambda_b}[\text{ps}]$	$m_{B_d}[\text{MeV}]$	$m_{B_s}[\text{MeV}]$	$m_{\Lambda_b}[\text{MeV}]$	[62, 66]
1.520 ± 0.004	1.505 ± 0.004	1.466 ± 0.010	5279.61	5366.79	5619.51	

$B \to D^{(*)}$ transition form factors						
	$F(1)|V_{cb}|[10^{-3}]$	ρ^2	R_1	R_2	R_3	
$B \to D$	42.65 ± 1.53	1.185 ± 0.054	—	—	—	[66, 67]
$B \to D^*$	35.81 ± 0.45	1.207 ± 0.026	1.406 ± 0.033	0.853 ± 0.020	0.97 ± 0.10	[66, 68]

$B_s \to D_s^{(*)}$ transition form factors						
	F_+	F_0	A_0	A_1	A_2	
$F(0)$	0.7 ± 0.1	0.7 ± 0.1	0.52 ± 0.06	0.62 ± 0.01	0.75 ± 0.07	[69]
$M_{\text{res}}[\text{GeV}]$	6.3	6.8	6.3	6.8	6.8	[69]

Light-meson decay constants and Gegenbauer moments						
	π	K	ρ	K^*	$a_1(1260)$	
$f_L[\text{MeV}]$	130.2 ± 1.4	155.6 ± 0.4	216 ± 6	211 ± 7	238 ± 10	[70–73]
α_1^L	—	-0.07 ± 0.04	—	-0.06 ± 0.04	—	
α_2^L	0.29 ± 0.08	0.24 ± 0.08	0.17 ± 0.07	0.16 ± 0.09	-0.02 ± 0.02	[71–74]

Table 1. Summary of theoretical input parameters. The Gegenbauer moments of light mesons are evaluated at $\mu = 1$ GeV.

factors is parameterized in a simplified z expansion [79], modified to account for pion-mass and lattice-spacing dependence. All relevant formulas and input data can be found in eq. (79) and tables VII–IX of [36]. Following the procedure recommended in [36], we calculate the central value, statistical uncertainty, and total systematic uncertainty of any observable depending on the form-factor parameters according to eqs. (82)–(84) in [36]. Furthermore, we have also taken into account the correlation matrices between the form-factor parameters.

The decay constants f_π and f_K are averaged over the two-flavour lattice QCD results [70], while f_ρ and f_{K^*} are determined from experiments [71]. The light-meson Gegenbauer moments are determined by the QCD sum rule approach [71, 72] and the lattice QCD calculation [74]. For the hadronic inputs of the axial-vector meson $a_1(1260)$, we use the results presented in ref. [73]. It is noted that the Gegenbauer moments are evaluated at $\mu = 1$ GeV, and are evolved to the characteristic scale $\mu \sim m_b$ [59–61]. We use LL running of the Gegenbauer moments for the tree-level and the one-loop amplitude, but NLL running in the two-loop amplitude. Moreover, the running of the Gegenbauer moments is performed in the four-flavour scheme.

6.2 Predictions for $a_1(D^{(*)+}L^-)$

We are now in the position to perform a numerical analysis of the coefficients $a_1(D^{(*)+}L^-)$ according to the expressions

$$a_1(D^+L^-) = \sum_{i=1}^{2} C_i(\mu) \int_0^1 du \left[\hat{T}_i(u,\mu) + \hat{T}_i'(u,\mu) \right] \Phi_L(u,\mu),$$

$$a_1(D^{*+}L^-) = \sum_{i=1}^{2} C_i(\mu) \int_0^1 du \left[\hat{T}_i(u,\mu) - \hat{T}_i'(u,\mu) \right] \Phi_L(u,\mu), \qquad (6.2)$$

into which eqs. (4.2) and (4.3) have to be inserted. Using the NNLO Wilson coefficients $C_i(\mu)$ in the CMM basis [42], together with the input parameters collected in table 1, our final numerical results for $a_1(D^+K^-)$ are given as

$$a_1(D^+K^-) = 1.025 + [0.029 + 0.018i]_{\text{NLO}} + [0.016 + 0.028i]_{\text{NNLO}}$$
$$= (1.069^{+0.009}_{-0.012}) + (0.046^{+0.023}_{-0.015})i, \qquad (6.3)$$

where the number without bracket is the LO contribution, which has no imaginary part, and the following two numbers are the NLO and NNLO terms, respectively. The total errors comprise the uncertainties, added in quadrature, from the variation of the scales $\mu \in [m_b/2, 2m_b]$ and $\mu_0 \in [m_W/2, 2m_W]$, the quark masses, the Gegenbauer moments, and $\alpha_s(m_Z)$. Unless stated otherwise, the numbers given here and below are obtained with the b- and c-quark masses renormalized in the pole scheme, which is set as our default scheme. It is observed that both the NLO and NNLO contributions add always constructively to the LO result. We also observe that the new two-loop correction is quite small in the real, but rather large in the imaginary part. It amounts to approximately 60% (2%) of the total imaginary (real) part of $a_1(D^+K^-)$. We emphasize that the sizable NNLO correction to the imaginary part does not indicate a breakdown of the perturbative expansion, but is due to the fact that the imaginary part vanishes at LO, and its NLO term is colour suppressed and proportional to the small Wilson coefficient $C_1(\mu)$. Moreover, the impact of the imaginary part on $|a_1(D^+K^-)|$ is only marginal. Graphical representations of $a_1(D^+K^-)$ are shown in figure 3 at LO, NLO and NNLO.

Due to the truncation of the perturbative expansion, the obtained values in eq. (6.3) depend on the renormalization scale μ, which is usually considered as a measure of the accuracy of the approximation at a given order in the perturbative expansion. This is
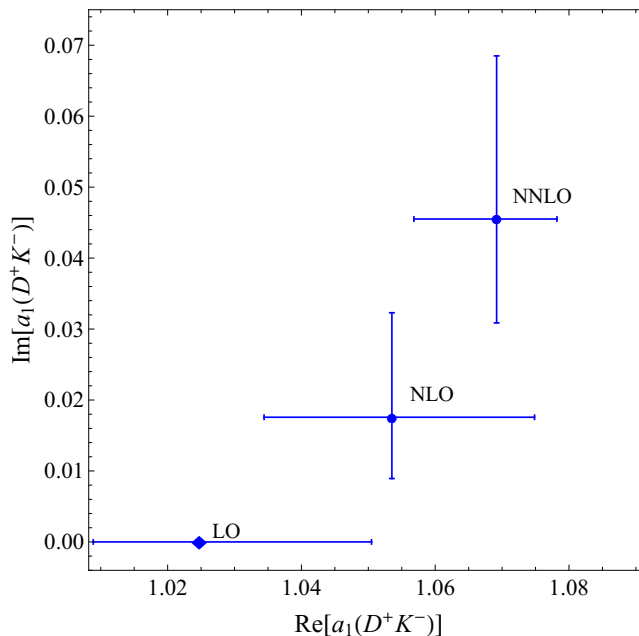
Figure 3. Graphical representation of $a_1(D^+K^-)$ in the complex plane at LO, NLO and NNLO. The theoretical error estimates are also indicated.
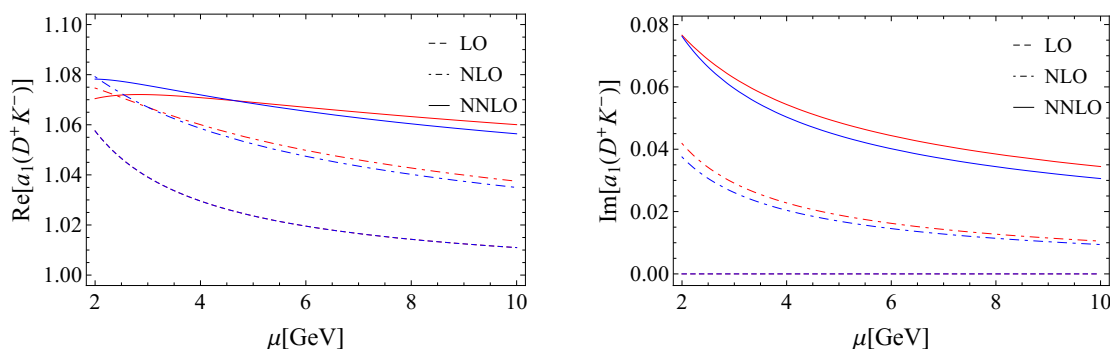
Figure 4. The dependence of the coefficient $a_1(D^+K^-)$ on the renormalization scale μ both in the pole (blue) and in the $\overline{\text{MS}}$ (red) scheme for b- and c-quark masses. Dashed, dashed-dotted and solid lines represent the LO, NLO, and NNLO results, respectively.

shown in figure 4 for $a_1(D^+K^-)$ up to NNLO, where results both in the pole (blue) and in the $\overline{\text{MS}}$ (red) scheme for b- and c-quark masses are given. We observe a pronounced stabilization of the scale dependence for the real part, but not for the imaginary part. This is again explained by the fact that the imaginary part vanishes at LO. It is also observed that the dependence on the b- and c-quark mass scheme is quite small, especially for the real part. We finally remark that also within a given quark-mass scheme the dependence of $a_1(D^+K^-)$ on the value of z_c is minor. The dependence of $a_1(D^+K^-)$ on the second Gegenbauer moment is small, too.

It is also interesting to mention that, even up to NNLO, the coefficients $a_1(D^{(*)+}L^-)$ are quasi-universal, with very small process-dependent non-factorizable corrections, a fact that was observed already at NLO in ref. [13]. This is clearly seen from the following

numerical results for different final states:

$$a_1(D^+K^-) = (1.069^{+0.009}_{-0.012}) + (0.046^{+0.023}_{-0.015})i \,,$$
$$a_1(D^+\pi^-) = (1.072^{+0.011}_{-0.013}) + (0.043^{+0.022}_{-0.014})i \,,$$
$$a_1(D^{*+}K^-) = (1.068^{+0.010}_{-0.012}) + (0.034^{+0.017}_{-0.011})i \,,$$
$$a_1(D^{*+}\pi^-) = (1.071^{+0.012}_{-0.013}) + (0.032^{+0.016}_{-0.010})i \,. \tag{6.4}$$

6.3 Predictions for class-I decays

It is generally believed that the factorization theorem is well established in class-I decays of the form $\bar{B}_{(s)} \to D_{(s)}^{(*)+}L^-$, where the spectator anti-quark of the initial $\bar{B}_{(s)}$ mesons is absorbed only by the $D_{(s)}^{(*)+}$ mesons [13, 80]. We now present in table 2 our predictions for the branching ratios of these decays through to NNLO. The explicit formulas for the branching ratios can be found in [13] and shall not be repeated here. The experimental data is taken from the Particle Data Group (PDG) [62] and/or the Heavy Flavor Averaging Group (HFAG) [66]. For the vector and axial-vector final states, the results refer to the longitudinal polarization amplitudes only, with the longitudinal polarization fractions taken from [81] for $\bar{B}_d \to D^{*+}\rho^-$ and [82] for $\bar{B}_s \to D_s^{*+}\rho^-$, respectively.

From table 2, one can see that our predictions for the branching ratios of these decays generally come out higher than the experimental data, especially for $\bar{B}_d \to D^{(*)+}\pi^-$ and $\bar{B}_d \to D^{(*)+}\rho^-$ decays, where the difference in central values is at the 20–30% level. Taking into account the uncertainties, the deviation is at the level of 2–3σ. Compared to ref. [13], which found at NLO rather good agreement between theory and experiment, essentially three things have changed: first, using the latest extraction from [66–68] our numerical values for the form factors are about 10% larger than the ones used in [13]. Second, the NNLO corrections add another positive shift of 2–3% on the amplitude level. Third, the experimental central values have slightly decreased since the analysis of [13]. All three effects shift theory and experiment further apart.

Given the fact that the results show rough agreement within errors for $\bar{B}_d \to D^{(*)+}K^{(*)-}$ decays, which receive only contributions from colour-allowed tree topologies, this may indicate a non-negligible impact from the W-exchange topologies appearing only in $\bar{B}_d \to D^{(*)+}\pi^-$ and $\bar{B}_d \to D^{(*)+}\rho^-$ decays. For $\bar{B}_s$ decays, on the other hand, since the $B_s \to D_s^{(*)}$ transition form factors have so far received only little theoretical attention [69, 83–88], especially by the lattice QCD community [78, 89], our theoretical predictions are still plagued by larger uncertainties due to these hadronic parameters.

6.4 Test of factorization

To further test the factorization hypothesis in class-I decays of B-mesons into heavy-light final states, as well as to probe the non-factorizable corrections to the coefficients $a_1(D^{(*)+}L^-)$, we now consider either ratios of non-leptonic to semi-leptonic decay rates [13, 17, 90, 91], or ratios of two non-leptonic decay rates [13, 91], both of which are essentially free of CKM and hadronic uncertainties.

As suggested firstly by Bjorken [90], a particularly clean and direct method to test the factorization hypothesis is provided by dividing the non-leptonic $\bar{B}_d \to D^{(*)+}L^-$ decay

Decay mode	LO	NLO	NNLO	Exp.
$\bar{B}_d \to D^+ \pi^-$	3.58	$3.79^{+0.44}_{-0.42}$	$3.93^{+0.43}_{-0.42}$	2.68 ± 0.13
$\bar{B}_d \to D^{*+} \pi^-$	3.15	$3.32^{+0.52}_{-0.49}$	$3.45^{+0.53}_{-0.50}$	2.76 ± 0.13
$\bar{B}_d \to D^+ \rho^-$	9.51	$10.06^{+1.25}_{-1.19}$	$10.42^{+1.24}_{-1.20}$	7.5 ± 1.2
$\bar{B}_d \to D^{*+} \rho^-$	8.45	$8.91^{+0.74}_{-0.71}$	$9.24^{+0.72}_{-0.71}$	6.0 ± 0.8
$\bar{B}_s \to D_s^+ \pi^-$	4.00	$4.24^{+1.32}_{-1.15}$	$4.39^{+1.36}_{-1.19}$	3.04 ± 0.23
$\bar{B}_s \to D_s^{*+} \pi^-$	2.05	$2.16^{+0.54}_{-0.49}$	$2.24^{+0.56}_{-0.50}$	2.0 ± 0.5
$\bar{B}_s \to D_s^+ \rho^-$	10.31	$10.91^{+3.46}_{-3.02}$	$11.30^{+3.56}_{-3.11}$	7.0 ± 1.5
$\bar{B}_s \to D_s^{*+} \rho^-$	5.86	$6.18^{+1.38}_{-1.28}$	$6.41^{+1.42}_{-1.31}$	10.2 ± 2.5
$\bar{B}_d \to D^+ K^-$	2.74	$2.90^{+0.33}_{-0.31}$	$3.01^{+0.32}_{-0.31}$	1.97 ± 0.21
$\bar{B}_d \to D^{*+} K^-$	2.37	$2.50^{+0.39}_{-0.36}$	$2.59^{+0.39}_{-0.37}$	2.14 ± 0.16
$\bar{B}_d \to D^+ K^{*-}$	4.79	$5.07^{+0.65}_{-0.62}$	$5.25^{+0.65}_{-0.63}$	4.5 ± 0.7
$\bar{B}_d \to D^{*+} K^{*-}$	4.30	$4.54^{+0.41}_{-0.40}$	$4.70^{+0.40}_{-0.39}$	—
$\bar{B}_s \to D_s^+ K^-$	3.05	$3.23^{+1.01}_{-0.88}$	$3.34^{+1.04}_{-0.90}$	—
$\bar{B}_s \to D_s^{*+} K^-$	1.53	$1.61^{+0.40}_{-0.36}$	$1.67^{+0.42}_{-0.37}$	—
$\bar{B}_s \to D_s^+ K^{*-}$	5.15	$5.45^{+1.74}_{-1.52}$	$5.64^{+1.79}_{-1.56}$	—
$\bar{B}_s \to D_s^{*+} K^{*-}$	3.02	$3.19^{+0.71}_{-0.65}$	$3.31^{+0.72}_{-0.67}$	—
$\bar{B}_d \to D^+ a_1^-$	10.82	$11.44^{+1.55}_{-1.48}$	$11.84^{+1.55}_{-1.50}$	6.0 ± 3.3
$\bar{B}_d \to D^{*+} a_1^-$	10.12	$10.66^{+1.11}_{-1.06}$	$11.06^{+1.10}_{-1.07}$	—
$\bar{B}_s \to D_s^+ a_1^-$	11.23	$11.87^{+3.84}_{-3.36}$	$12.29^{+3.95}_{-3.46}$	—
$\bar{B}_s \to D_s^{*+} a_1^-$	7.44	$7.84^{+1.64}_{-1.53}$	$8.13^{+1.68}_{-1.57}$	—

Table 2. CP-averaged branching ratios (in units of 10^{-3} for $b \to c\bar{u}d$ and 10^{-4} for $b \to c\bar{u}s$ transitions) of $\bar{B}_{(s)} \to D_{(s)}^{(*)+} L^-$ decays. The vector- and axial-vector final states refer to the longitudinal polarization amplitudes only. The theoretical errors shown correspond to the uncertainties due to renormalization scales μ and μ_0, the CKM as well as the hadronic parameters, added in quadrature. The experimental data is taken from refs. [62, 66, 81, 82].

rates by the corresponding differential semi-leptonic $\bar{B}_d \to D^{(*)+} \ell^- \bar{\nu}_\ell$ decay rates evaluated at $q^2 = m_L^2$, where ℓ refers to either an electron or a muon, and q^2 is the four-momentum squared transferring to the lepton pair. In this way, the coefficients $a_1(D^{(*)+} L^-)$ can be extracted directly from experimental data through the relation [13, 91]

$$R_L^{(*)} \equiv \frac{\Gamma(\bar{B}_d \to D^{(*)+} L^-)}{d\Gamma(\bar{B}_d \to D^{(*)+} \ell^- \bar{\nu}_\ell)/dq^2 \big|_{q^2 = m_L^2}} = 6\pi^2 \, |V_{ij}|^2 \, f_L^2 \, |a_1(D^{(*)+} L^-)|^2 \, X_L^{(*)}, \quad (6.5)$$

where V_{ij} is, depending on the constituent quark content of the meson L, the appropriate CKM matrix element. With the light lepton mass neglected, $X_L = X_L^* = 1$ for a vector or

$|a_1(D^{(*)+}L^-)|$	LO	NLO	NNLO	Exp.
$|a_1(D^+\pi^-)|$	1.025	$1.054^{+0.022}_{-0.020}$	$1.073^{+0.012}_{-0.014}$	0.89 ± 0.05
$|a_1(D^{*+}\pi^-)|$	1.025	$1.052^{+0.020}_{-0.018}$	$1.071^{+0.013}_{-0.014}$	0.96 ± 0.03
$|a_1(D^+\rho^-)|$	1.025	$1.054^{+0.022}_{-0.019}$	$1.072^{+0.012}_{-0.014}$	0.91 ± 0.08
$|a_1(D^{*+}\rho^-)|$	1.025	$1.052^{+0.020}_{-0.018}$	$1.071^{+0.013}_{-0.014}$	0.86 ± 0.06
$|a_1(D^+K^-)|$	1.025	$1.054^{+0.022}_{-0.019}$	$1.070^{+0.010}_{-0.013}$	0.87 ± 0.06
$|a_1(D^{*+}K^-)|$	1.025	$1.052^{+0.020}_{-0.018}$	$1.069^{+0.010}_{-0.013}$	0.97 ± 0.04
$|a_1(D^+K^{*-})|$	1.025	$1.054^{+0.022}_{-0.019}$	$1.070^{+0.010}_{-0.013}$	0.99 ± 0.09
$|a_1(D^+a_1^-)|$	1.025	$1.054^{+0.022}_{-0.019}$	$1.072^{+0.012}_{-0.014}$	0.76 ± 0.19

Table 3. Theoretical predictions for $|a_1(D^{(*)+}L^-)|$ at different orders in perturbation theory. For comparison, the coefficients $|a_1(D^{(*)+}L^-)|$ determined from current data are shown in the last column. The experimental errors are estimated by adding the uncertainties of the non-leptonic branching ratios and the semi-leptonic decay rates in quadrature, while the uncertainties from the decay constants are not taken into account.

axis-vector meson, whereas for a pseudoscalar $X_L^{(*)}$ deviates from unity only by calculable terms of order m_L^2/m_B^2, which are numerically below the percent level; explicit expressions for $X_L^{(*)}$ can be found, for example, in ref. [91]. To get the differential semi-leptonic decay rates at $q^2 = m_L^2$ in eq. (6.5), we use the CLN parameterization for the $B \to D^{(*)}$ transition form factors [76], with the relevant parameters summarized in table 1. Explicitly, we get numerically (in units of 10^{-3} GeV^{-2} ps^{-1})

$$\frac{d\Gamma(\bar{B}_d \to D^{(*)+}\ell^-\bar{\nu}_\ell)}{dq^2}\bigg|_{q^2=m_L^2} = \begin{cases} 2.35^{+0.25}_{-0.24} \ (2.04 \pm 0.10), & \text{for } L = \pi^- \\ 2.27^{+0.23}_{-0.22} \ (2.28 \pm 0.10), & \text{for } L = \rho^- \\ 2.32^{+0.24}_{-0.23} \ (2.14 \pm 0.10), & \text{for } L = K^- \\ 2.24^{+0.23}_{-0.22} \ (2.36 \pm 0.10), & \text{for } L = K^{*-} \\ 2.13^{+0.21}_{-0.20} \ (2.64 \pm 0.11), & \text{for } L = a_1^- \end{cases} \tag{6.6}$$

Together with the data on the branching ratios of non-leptonic decays given in table 2, we arrive at the experimental values for $|a_1(D^{(*)+}L^-)|$ collected in table 3, where, for comparison, our theoretical predictions at different orders are also shown.

From table 3, one can see clearly that our theoretical predictions based on the QCDF approach result in an essentially universal value of $|a_1(D^{(*)+}L^-)| \simeq 1.07$ (1.05) at NNLO (NLO), being consistently higher than the central values favoured by the current experimental data. The deviation is again at the level of 2–3σ. Similar results were obtained in [17], yet without inclusion of the NNLO correction. It would be, therefore, very encouraging to determine directly the ratios of non-leptonic and semi-leptonic decay rates at current and future experiments such as LHCb and Belle II. Compared to the NLO analysis in [13], where theory predictions for $|a_1(D^{(*)+}L^-)|$ were found to be in agreement

Ratios	LO	NLO	NNLO	Exp.
$\frac{\mathrm{Br}(\bar{B}_d \to D^{*+}\pi^-)}{\mathrm{Br}(\bar{B}_d \to D^+\pi^-)}$	0.880	$0.876^{+0.162}_{-0.150}$	$0.878^{+0.162}_{-0.150}$	1.03 ± 0.07
$\frac{\mathrm{Br}(\bar{B}_d \to D^+\rho^-)}{\mathrm{Br}(\bar{B}_d \to D^+\pi^-)}$	2.654	$2.653^{+0.163}_{-0.158}$	$2.653^{+0.163}_{-0.158}$	2.80 ± 0.47
$\frac{\mathrm{Br}(\bar{B}_d \to D^+\rho^-)}{\mathrm{Br}(\bar{B}_d \to D^{*+}\pi^-)}$	3.016	$3.027^{+0.599}_{-0.531}$	$3.022^{+0.598}_{-0.530}$	2.72 ± 0.45
$\frac{\mathrm{Br}(\bar{B}_d \to D^{*+}K^-)}{\mathrm{Br}(\bar{B}_d \to D^+K^-)}$	0.865	$0.862^{+0.158}_{-0.147}$	$0.863^{+0.158}_{-0.147}$	1.086 ± 0.141
$\frac{\mathrm{Br}(\bar{B}_d \to D^+K^{*-})}{\mathrm{Br}(\bar{B}_d \to D^+K^-)}$	1.747	$1.746^{+0.118}_{-0.115}$	$1.746^{+0.118}_{-0.115}$	2.284 ± 0.431
$\frac{\mathrm{Br}(\bar{B}_d \to D^+K^{*-})}{\mathrm{Br}(\bar{B}_d \to D^{*+}K^-)}$	2.019	$2.026^{+0.404}_{-0.358}$	$2.023^{+0.403}_{-0.358}$	2.103 ± 0.363
$\frac{\mathrm{Br}(\bar{B}_d \to D^+K^-)}{\mathrm{Br}(\bar{B}_d \to D^+\pi^-)}$	0.077	$0.077^{+0.002}_{-0.002}$	$0.077^{+0.002}_{-0.002}$	0.074 ± 0.009
$\frac{\mathrm{Br}(\bar{B}_d \to D^{*+}K^-)}{\mathrm{Br}(\bar{B}_d \to D^{*+}\pi^-)}$	0.075	$0.075^{+0.002}_{-0.002}$	$0.075^{+0.002}_{-0.002}$	0.078 ± 0.007
$\frac{\mathrm{Br}(\bar{B}_d \to D^+K^{*-})}{\mathrm{Br}(\bar{B}_d \to D^+\rho^-)}$	0.050	$0.050^{+0.005}_{-0.004}$	$0.050^{+0.005}_{-0.004}$	0.060 ± 0.013
$\frac{\mathrm{Br}(\bar{B}_s \to D_s^+\pi^-)}{\mathrm{Br}(\bar{B}_d \to D^+K^-)}$	14.67	$14.67^{+1.34}_{-1.28}$	$14.67^{+1.34}_{-1.28}$	15.43 ± 2.02
$\frac{\mathrm{Br}(\bar{B}_s \to D_s^+\pi^-)}{\mathrm{Br}(\bar{B}_d \to D^+\pi^-)}$	1.120	$1.120^{+0.109}_{-0.104}$	$1.120^{+0.109}_{-0.104}$	1.134 ± 0.102

Table 4. Predictions for the ratios of non-leptonic $\bar{B}_{(s)} \to D^{(*)+}_{(s)} L^-$ decay rates at different orders. The experimental data is obtained using the corresponding branching fractions collected in table 2.

with the values extracted from experiment, together with the conclusion that there was no hint for sizable power corrections, the situation has changed, owing to increased values in the theory predictions and, at the same time, decreased experimental values (see also the discussion in section 6.3). We will come back to this point below.

We now turn to discuss the ratios of non-leptonic $\bar{B}_{(s)} \to D^{(*)+}_{(s)} L^-$ decay rates, following the notations used in refs. [13, 91]. As a quasi-universal $|a_1(D^{(*)+}L^-)|$ is predicted in the QCDF approach, these ratios could be used to test the factorization hypothesis, as well as the SU(3) relations in B-meson decays into heavy-light final states [17]. Our results of such an analysis are presented in table 4, where the experimental data is obtained using the corresponding branching fractions collected in table 2.

From table 4, one can see that, within the errors, our theoretical predictions are generally consistent with the current experimental data, indicating therefore no evidence for any significant deviation from the factorization hypothesis for these class-I B-meson decays into heavy-light final states. The last two ratios shown in table 4 could also be used to determine the ratio of fragmentation functions f_d/f_s, a key quantity for precise measurements of absolute B_s-meson decay rates at hadron colliders [17, 92].

One possible interpretation of our findings that, on the one hand, the non-leptonic to semi-leptonic ratios come out larger in theory compared to experiment, and on the other hand the non-leptonic ratios in general agree with experiment, might be non-negligible power corrections which could be negative in sign and 10–15% in size on the amplitude level. They would render the factorization test via non-leptonic to semi-leptonic ratios

better, and at the same time could cancel out in the non-leptonic ratios, especially if they were of a certain universality. The size of power corrections stemming from spectator scattering and weak annihilation was roughly estimated in section 6.5 of [13]. Depending on the phases of the integrals over the D-meson wave function and on the value of the first inverse moment λ_B of the B-meson distribution amplitude, these two contributions could in principle interfere constructively, and in this case their total effect could indeed add up to -10% in the amplitude.

Another possibility which has essentially the same effect would be to reduce the values of $|V_{cb}|$ times the form factors by $\sim 10\%$. This option seems attractive in view of the fact that those non-leptonic ratios in table 4 in which $|V_{cb}|$ and the form factors cancel out are in very good agreement with experiment. On the other hand, the semi-leptonic rate is measured very precisely and the current form factors times $|V_{cb}|$ are extracted by HFAG [66] from a global fit to all available data, whose result we quote in table 1. Hence they are optimized to describe the shape of the semi-leptonic rate and therefore should be trustworthy. One could even conclude from this that the experimental extraction of $|a_1(D^{(*)+}L^-)|$ from eq. (6.5) is independent of the product of $|V_{cb}|$ and the form factor.

We emphasize that without a rigorous treatment of power corrections in the QCDF approach nothing more can be said at the present stage. In any case, the QCDF approach per se is not invalidated.

6.5 Predictions for $\Lambda_b \to \Lambda_c^+ L^-$ decays

While the Λ_b baryons are not produced at an e^+e^- B-factory, they account for about 20% of the b-hadrons produced at the LHC [93]. Remarkably, the number of Λ_b baryons produced is comparable to the number of B_u or B_d mesons, and is significantly higher than the number of B_s mesons. Due to the half-integer-spin of Λ_b, its decays provide complementary information compared to the corresponding mesonic ones. Therefore, this may open up a new field for flavour physics. For a review, see e.g. refs. [94–97]. Here we study the two-body non-leptonic $\Lambda_b \to \Lambda_c^+ L^-$ decays, for which the factorization assumption is believed to be reliable [37, 98–101]. As demonstrated especially in ref. [37], the proof of factorization at leading order in $\Lambda_{\text{QCD}}/m_{b,c}$ for these decays follows closely that for $\bar{B}_d \to D^{(*)+}\pi^-$ [80]. These decays provide, therefore, a testing ground for different QCD models and factorization assumptions used in B-meson case. It is straightforward to generalize the expressions in [37] to take radiative corrections through to NNLO into account.

Using the most recent lattice QCD results for $\Lambda_b \to \Lambda_c$ transition form factors [36], we present in table 5 our predictions for the branching fractions of $\Lambda_b \to \Lambda_c^+ L^-$ decays, as well as some ratios between them, where the experimental data is taken from HFAG [66]. From table 5, one can see that, contrary to the observation made in mesonic decays, our predictions for the branching ratios of these decays now come out lower than the experimental data; especially the higher-order corrections always increase the LO predictions and shift our predictions closer to the experimental data. Our predictions for the two ratios $\text{Br}(\Lambda_b \to \Lambda_c^+ \mu^- \bar{\nu})/\text{Br}(\Lambda_b \to \Lambda_c^+ \pi^-)$ and $\text{Br}(\Lambda_b \to \Lambda_c^+ K^-)/\text{Br}(\Lambda_b \to \Lambda_c^+ \pi^-)$ are both consistent with the current data, indicating that the non-factorizable effects should be small in these decays. Moreover, we emphasize the fact that the non-leptonic to semi-leptonic ratio

Decay mode	LO	NLO	NNLO	Exp.
$\Lambda_b \to \Lambda_c^+ \pi^-$	2.60	$2.75^{+0.53}_{-0.53}$	$2.85^{+0.54}_{-0.54}$	$4.30^{+0.36}_{-0.35}$
$\Lambda_b \to \Lambda_c^+ \rho^-$	7.46	$7.88^{+1.44}_{-1.43}$	$8.17^{+1.47}_{-1.47}$	—
$\Lambda_b \to \Lambda_c^+ a_1^-$	9.57	$10.11^{+1.75}_{-1.72}$	$10.47^{+1.78}_{-1.77}$	—
$\Lambda_b \to \Lambda_c^+ K^-$	2.02	$2.14^{+0.40}_{-0.39}$	$2.21^{+0.40}_{-0.40}$	3.42 ± 0.33
$\Lambda_b \to \Lambda_c^+ K^{*-}$	3.86	$4.07^{+0.74}_{-0.73}$	$4.22^{+0.75}_{-0.75}$	—
$\frac{\mathrm{Br}(\Lambda_b \to \Lambda_c^+ \mu^- \bar{\nu})}{\mathrm{Br}(\Lambda_b \to \Lambda_c^+ \pi^-)}$	18.88	$17.87^{+2.31}_{-2.33}$	$17.25^{+2.19}_{-2.18}$	$16.6^{+4.1}_{-4.7}$
$\frac{\mathrm{Br}(\Lambda_b \to \Lambda_c^+ K^-)}{\mathrm{Br}(\Lambda_b \to \Lambda_c^+ \pi^-)}$ (%)	7.77	$7.77^{+0.19}_{-0.18}$	$7.77^{+0.19}_{-0.18}$	7.31 ± 0.23
$\frac{\mathrm{Br}(\Lambda_b \to \Lambda_c^+ \pi^-)}{\mathrm{Br}(\bar{B}_d \to D^+ \pi^-)}$	0.73	$0.73^{+0.16}_{-0.15}$	$0.73^{+0.16}_{-0.15}$	3.3 ± 1.2

Table 5. Predictions for the branching fractions (in units of 10^{-3} for $b \to c\bar{u}d$ and 10^{-4} for $b \to c\bar{u}s$ transitions) of $\Lambda_b \to \Lambda_c^+ L^-$ decays, as well as some ratios between them. The experimental data is taken from PDG [62] and HFAG [66].

in the baryonic case is consistent with experiment, but shows a tension in the mesonic case (see section 6.4). The discrepancy between our prediction and the current experimental data for $\mathrm{Br}(\Lambda_b \to \Lambda_c^+ \pi^-)/\mathrm{Br}(\bar{B}_d \to D^+ \pi^-)$ makes it interesting to evaluate directly the form-factor ratios of $\Lambda_b \to \Lambda_c$ and $B \to D$ transitions by the lattice community.

7 Conclusion

We have calculated the NNLO vertex corrections to the colour-allowed tree topology in the framework of QCDF for the mesonic decays $\bar{B}_{(s)} \to D_{(s)}^{(*)+} L^-$ and the baryonic decays $\Lambda_b \to \Lambda_c^+ L^-$, with $L = \{\pi, \rho, K^{(*)}, a_1\}$. The calculation of the two-loop correction to the hard scattering kernels requires the evaluation of several dozens of genuine two-scale Feynman diagrams, which describe these heavy-to-heavy transitions at the quark level. We performed this calculation by means of techniques that have become standard in the business of multi-loop computations. It might be worth noting that we evaluated all master integrals analytically [33] in a so-called canonical basis [50], a result which catalyzed the convolution with the LCDA and enabled us to obtain the convoluted kernels almost completely analytically.

The NNLO contributions yield a positive shift to the colour-allowed tree amplitude a_1, which is sizable for its imaginary part, but small for its real part and its magnitude. Moreover, the amplitude only mildly depends on the ratio of the heavy-quark masses $z_c = m_c^2/m_b^2$. The dependence on the factorization scale gets reduced for the real part compared to the NLO result. This reduction does not occur in the imaginary parts, which is expected, as the latter only arise beyond LO. We performed our analysis using the pole scheme for the heavy-quark masses. A change to the $\overline{\text{MS}}$ scheme does not show any significant shift of the amplitude within the range of physical values for the heavy-quark

masses. Moreover, the results for the different final states only slightly depend on the light meson LCDA and hence, we can confirm the quasi-universality of the tree amplitude to NNLO accuracy.

In our phenomenological analysis we evaluated the branching ratios to NNLO accuracy, and with the latest values for the non-perturbative input parameters. We find that for $\bar{B}_d$ decays the central values of the theoretical predictions are in general higher compared to the experimental values. Within the given uncertainties the quantities agree at the 2–3σ level for π and ρ in the final state, and slightly better for K and K^*. Compared to the analysis at NLO [13], our increased values for the form factors and the amplitude, together with decreased experimental values, have shifted theory and experiment further apart. For $\bar{B}_s$ decays, the theory predictions are still plagued by large uncertainties which are mainly due to poorly known form factors. For the baryonic decays, on the other hand, the predicted branching fractions turn out to be $20-30\%$ smaller than the experimental ones. It would be interesting to understand the reason for this difference in the $\bar{B}_d$ and the Λ_b decays. We therefore propose a systematic analysis of factorization for Λ_b decays in the future.

Moreover, we analyzed ratios of non-leptonic and semi-leptonic decay rates in order to further probe the factorization theorem to NNLO. The ratios of different non-leptonic rates turn out to be in good agreement, comparing theoretical prediction and experiment. In the case of non-leptonic to semi-leptonic ratios, on the other hand, the values for $|a_1(D^{(*)+}L^-)|$ that we extract from experiment are lower by 2–3σ compared to the NNLO theory predictions (see also [17]).

One possibility to interpret the entity of these results could be non-negligible power corrections. Given the uncertainties of the branching ratios and a_1 they could be negative in sign and 10–15% in size on the amplitude level. They could cure the non-leptonic to semi-leptonic ratios, without destroying the agreement in the non-leptonic ratios, especially if they were of a certain universality. It will also be very interesting to investigate what this would imply for the power corrections in charmless non-leptonic decays. Recent analyses that address weak annihilation in charmless non-leptonic decays can be found in [102–104].

Another, yet less favourable option would be reduced values of $|V_{cb}|$ times the form factors. As stated already in section 6, without a rigorous treatment of power corrections in the QCDF approach nothing more can be said at the present stage.

Acknowledgments

References

[1] M. Artuso et al., *B, D and K decays*, *Eur. Phys. J.* **C 57** (2008) 309 [arXiv:0801.1833] [inSPIRE].

[2] M. Antonelli et al., *Flavor physics in the quark sector*, *Phys. Rept.* **494** (2010) 197 [arXiv:0907.5386] [inSPIRE].

[3] LHCb collaboration, *Measurement of CP observables in $B^{\pm} \to DK^{\pm}$ and $B^{\pm} \to D\pi^{\pm}$ with two- and four-body D decays*, *Phys. Lett.* **B 760** (2016) 117 [arXiv:1603.08993] [inSPIRE].

[4] BELLE, BaBar collaboration, A.J. Bevan et al., *The physics of the B factories*, *Eur. Phys. J.* **C 74** (2014) 3026 [arXiv:1406.6311] [inSPIRE].

[5] LHCb collaboration, *Determination of the branching fractions of $B^0_S \to D^{\mp}_S K^{\mp}$ and $B^0 \to D^-_S K^+$*, *JHEP* **05** (2015) 019 [arXiv:1412.7654] [inSPIRE].

[6] LHCb collaboration, *First observation and measurement of the branching fraction for the decay $B^0_s \to D^{*\mp}_s K^{\pm}$*, *JHEP* **06** (2015) 130 [arXiv:1503.09086] [inSPIRE].

[7] T. Aushev et al., *Physics at Super B Factory*, arXiv:1002.5012 [inSPIRE].

[8] M. Bauer, B. Stech and M. Wirbel, *Exclusive nonleptonic decays of D, D(s) and B mesons*, *Z. Phys.* **C 34** (1987) 103 [inSPIRE].

[9] D. Zeppenfeld, SU(3) *relations for B meson decays*, *Z. Phys.* **C 8** (1981) 77 [inSPIRE].

[10] Y.-Y. Keum, H.-n. Li and A.I. Sanda, *Fat penguins and imaginary penguins in perturbative QCD*, *Phys. Lett.* **B 504** (2001) 6 [hep-ph/0004004] [inSPIRE].

[11] Y.Y. Keum, H.-N. Li and A.I. Sanda, *Penguin enhancement and $B \to K\pi$ decays in perturbative QCD*, *Phys. Rev.* **D 63** (2001) 054008 [hep-ph/0004173] [inSPIRE].

[12] M. Beneke, G. Buchalla, M. Neubert and C.T. Sachrajda, *QCD factorization for $B \to \pi\pi$ decays: strong phases and CP-violation in the heavy quark limit*, *Phys. Rev. Lett.* **83** (1999) 1914 [hep-ph/9905312] [inSPIRE].

[13] M. Beneke, G. Buchalla, M. Neubert and C.T. Sachrajda, *QCD factorization for exclusive, nonleptonic B meson decays: general arguments and the case of heavy light final states*, *Nucl. Phys.* **B 591** (2000) 313 [hep-ph/0006124] [inSPIRE].

[14] M. Beneke, G. Buchalla, M. Neubert and C.T. Sachrajda, *QCD factorization in $B \to \pi K$, $\pi\pi$ decays and extraction of Wolfenstein parameters*, *Nucl. Phys.* **B 606** (2001) 245 [hep-ph/0104110] [inSPIRE].

[15] S.-H. Zhou, Y.-B. Wei, Q. Qin, Y. Li, F.-S. Yu and C.-D. Lu, *Analysis of two-body charmed B meson decays in factorization-assisted topological-amplitude approach*, *Phys. Rev.* **D 92** (2015) 094016 [arXiv:1509.04060] [inSPIRE].

[16] M. Beneke and M. Neubert, *QCD factorization for $B \to PP$ and $B \to PV$ decays*, *Nucl. Phys.* **B 675** (2003) 333 [hep-ph/0308039] [inSPIRE].

[17] R. Fleischer, N. Serra and N. Tuning, *Tests of factorization and* SU(3) *relations in B decays into heavy-light final states*, *Phys. Rev.* **D 83** (2011) 014017 [arXiv:1012.2784] [inSPIRE].

[18] X.-q. Li and Y.-d. Yang, *Revisiting $B \to \pi\pi$, πK decays in QCD factorization approach*, *Phys. Rev.* **D 72** (2005) 074007 [hep-ph/0508079] [inSPIRE].

[19] M. Beneke and S. Jager, *Spectator scattering at NLO in non-leptonic b decays: tree amplitudes*, *Nucl. Phys.* **B 751** (2006) 160 [hep-ph/0512351] [INSPIRE].

[20] X.-q. Li and Y.-d. Yang, *Reexamining charmless $B \to PV$ decays in QCD factorization approach*, *Phys. Rev.* **D 73** (2006) 114027 [hep-ph/0602224] [INSPIRE].

[21] N. Kivel, *Radiative corrections to hard spectator scattering in $B \to \pi\pi$ decays*, *JHEP* **05** (2007) 019 [hep-ph/0608291] [INSPIRE].

[22] M. Beneke and S. Jager, *Spectator scattering at NLO in non-leptonic B decays: leading penguin amplitudes*, *Nucl. Phys.* **B 768** (2007) 51 [hep-ph/0610322] [INSPIRE].

[23] A. Jain, I.Z. Rothstein and I.W. Stewart, *Penguin loops for nonleptonic B-decays in the standard model: is there a penguin puzzle?*, arXiv:0706.3399 [INSPIRE].

[24] V. Pilipp, *Hard spectator interactions in $B \to \pi\pi$ at order α_s^2*, *Nucl. Phys.* **B 794** (2008) 154 [arXiv:0709.3214] [INSPIRE].

[25] G. Bell, *NNLO vertex corrections in charmless hadronic B decays: imaginary part*, *Nucl. Phys.* **B 795** (2008) 1 [arXiv:0705.3127] [INSPIRE].

[26] G. Bell, *NNLO vertex corrections in charmless hadronic B decays: real part*, *Nucl. Phys.* **B 822** (2009) 172 [arXiv:0902.1915] [INSPIRE].

[27] G. Bell and V. Pilipp, $B^- \to \pi^- \pi^0/\rho^- \rho^0$ *to NNLO in QCD factorization*, *Phys. Rev.* **D 80** (2009) 054024 [arXiv:0907.1016] [INSPIRE].

[28] M. Beneke, T. Huber and X.-Q. Li, *NNLO vertex corrections to non-leptonic B decays: tree amplitudes*, *Nucl. Phys.* **B 832** (2010) 109 [arXiv:0911.3655] [INSPIRE].

[29] C.S. Kim and Y.W. Yoon, *Order α_s^2 magnetic penguin correction for B decay to light mesons*, *JHEP* **11** (2011) 003 [arXiv:1107.1601] [INSPIRE].

[30] G. Bell and T. Huber, *Master integrals for the two-loop penguin contribution in non-leptonic B-decays*, *JHEP* **12** (2014) 129 [arXiv:1410.2804] [INSPIRE].

[31] G. Bell, M. Beneke, T. Huber and X.-Q. Li, *Two-loop current-current operator contribution to the non-leptonic QCD penguin amplitude*, *Phys. Lett.* **B 750** (2015) 348 [arXiv:1507.03700] [INSPIRE].

[32] T. Huber and S. Kränkl, *Towards NNLO corrections in $B \to D\pi$*, arXiv:1405.5911 [INSPIRE].

[33] T. Huber and S. Kränkl, *Two-loop master integrals for non-leptonic heavy-to-heavy decays*, *JHEP* **04** (2015) 140 [arXiv:1503.00735] [INSPIRE].

[34] Q. Chang, L.-X. Chen, Y.-Y. Zhang, J.-F. Sun and Y.-L. Yang, $\bar{B}_{d,s} \to D^*_{d,s}V$ *and* $\bar{B}^*_{d,s} \to D_{d,s}V$ *decays with QCD factorization and possible puzzles*, arXiv:1605.01631 [INSPIRE].

[35] LHCb collaboration, *Studies of beauty baryon decays to $D^0 p h^-$ and $\Lambda_c^+ h^-$ final states*, *Phys. Rev.* **D 89** (2014) 032001 [arXiv:1311.4823] [INSPIRE].

[36] W. Detmold, C. Lehner and S. Meinel, $\Lambda_b \to p\ell^-\bar{\nu}_\ell$ *and* $\Lambda_b \to \Lambda_c \ell^- \bar{\nu}_\ell$ *form factors from lattice QCD with relativistic heavy quarks*, *Phys. Rev.* **D 92** (2015) 034503 [arXiv:1503.01421] [INSPIRE].

[37] A.K. Leibovich, Z. Ligeti, I.W. Stewart and M.B. Wise, *Predictions for nonleptonic Λ_b and Θ_b decays*, *Phys. Lett.* **B 586** (2004) 337 [hep-ph/0312319] [INSPIRE].

[38] G. Buchalla, A.J. Buras and M.E. Lautenbacher, *Weak decays beyond leading logarithms*, *Rev. Mod. Phys.* **68** (1996) 1125 [hep-ph/9512380] [INSPIRE].

[39] K.G. Chetyrkin, M. Misiak and M. Münz, *Weak radiative B meson decay beyond leading logarithms*, *Phys. Lett.* **B 400** (1997) 206 [*Erratum ibid.* **B 425** (1998) 414] [hep-ph/9612313] [INSPIRE].

[40] K.G. Chetyrkin, M. Misiak and M. Münz, $|\Delta F| = 1$ *nonleptonic effective Hamiltonian in a simpler scheme*, *Nucl. Phys.* **B 520** (1998) 279 [hep-ph/9711280] [INSPIRE].

[41] P. Gambino, M. Gorbahn and U. Haisch, *Anomalous dimension matrix for radiative and rare semileptonic B decays up to three loops*, *Nucl. Phys.* **B 673** (2003) 238 [hep-ph/0306079] [INSPIRE].

[42] M. Gorbahn and U. Haisch, *Effective Hamiltonian for non-leptonic* $|\Delta F| = 1$ *decays at NNLO in QCD*, *Nucl. Phys.* **B 713** (2005) 291 [hep-ph/0411071] [INSPIRE].

[43] M. Neubert, *Heavy quark symmetry*, *Phys. Rept.* **245** (1994) 259 [hep-ph/9306320] [INSPIRE].

[44] G. Passarino and M.J.G. Veltman, *One loop corrections for* e^+e^- *annihilation into* $\mu^+\mu^-$ *in the Weinberg model*, *Nucl. Phys.* **B 160** (1979) 151 [INSPIRE].

[45] S. Laporta and E. Remiddi, *The analytical value of the electron* $(g-2)$ *at order* α^3 *in QED*, *Phys. Lett.* **B 379** (1996) 283 [hep-ph/9602417] [INSPIRE].

[46] S. Laporta, *High precision calculation of multiloop Feynman integrals by difference equations*, *Int. J. Mod. Phys.* **A 15** (2000) 5087 [hep-ph/0102033] [INSPIRE].

[47] K.G. Chetyrkin and F.V. Tkachov, *Integration by parts: the algorithm to calculate* β-*functions in* 4 *loops*, *Nucl. Phys.* **B 192** (1981) 159 [INSPIRE].

[48] C. Anastasiou and A. Lazopoulos, *Automatic integral reduction for higher order perturbative calculations*, *JHEP* **07** (2004) 046 [hep-ph/0404258] [INSPIRE].

[49] A.V. Smirnov, *Algorithm FIRE — Feynman Integral REduction*, *JHEP* **10** (2008) 107 [arXiv:0807.3243] [INSPIRE].

[50] J.M. Henn, *Multiloop integrals in dimensional regularization made simple*, *Phys. Rev. Lett.* **110** (2013) 251601 [arXiv:1304.1806] [INSPIRE].

[51] A.B. Goncharov, *Multiple polylogarithms, cyclotomy and modular complexes*, *Math. Res. Lett.* **5** (1998) 497 [arXiv:1105.2076] [INSPIRE].

[52] A.V. Efremov and A.V. Radyushkin, *Factorization and asymptotical behavior of pion form-factor in QCD*, *Phys. Lett.* **B 94** (1980) 245 [INSPIRE].

[53] G.P. Lepage and S.J. Brodsky, *Exclusive processes in perturbative quantum chromodynamics*, *Phys. Rev.* **D 22** (1980) 2157 [INSPIRE].

[54] M. Beneke and D. Yang, *Heavy-to-light B meson form-factors at large recoil energy: spectator-scattering corrections*, *Nucl. Phys.* **B 736** (2006) 34 [hep-ph/0508250] [INSPIRE].

[55] E. Remiddi and J.A.M. Vermaseren, *Harmonic polylogarithms*, *Int. J. Mod. Phys.* **A 15** (2000) 725 [hep-ph/9905237] [INSPIRE].

[56] J. Vollinga and S. Weinzierl, *Numerical evaluation of multiple polylogarithms*, *Comput. Phys. Commun.* **167** (2005) 177 [hep-ph/0410259] [INSPIRE].

[57] D. Maître, *HPL, a Mathematica implementation of the harmonic polylogarithms*, *Comput. Phys. Commun.* **174** (2006) 222 [hep-ph/0507152] [INSPIRE].

[58] D. Maître, *Extension of HPL to complex arguments*, *Comput. Phys. Commun.* **183** (2012) 846 [hep-ph/0703052] [INSPIRE].

[59] D. Mueller, *Conformal constraints and the evolution of the nonsinglet meson distribution amplitude*, *Phys. Rev.* **D 49** (1994) 2525 [INSPIRE].

[60] S.V. Mikhailov and A.V. Radyushkin, *Evolution kernels in QCD: two loop calculation in Feynman gauge*, *Nucl. Phys.* **B 254** (1985) 89 [INSPIRE].

[61] D. Mueller, *The Evolution of the pion distribution amplitude in next-to-leading-order*, *Phys. Rev.* **D 51** (1995) 3855 [hep-ph/9411338] [INSPIRE].

[62] PARTICLE DATA GROUP collaboration, K.A. Olive et al., *Review of particle physics*, *Chin. Phys.* **C 38** (2014) 090001 [INSPIRE].

[63] ATLAS, CDF, CMS, D0 collaboration, *First combination of Tevatron and LHC measurements of the top-quark mass*, arXiv:1403.4427 [INSPIRE].

[64] J.C. Hardy and I.S. Towner, *Superallowed $0^+ \to 0^+$ nuclear β decays: 2014 critical survey, with precise results for V_{ud} and CKM unitarity*, *Phys. Rev.* **C 91** (2015) 025501 [arXiv:1411.5987] [INSPIRE].

[65] CKMFITTER GROUP collaboration, J. Charles et al., *CP violation and the CKM matrix: assessing the impact of the asymmetric B factories*, *Eur. Phys. J.* **C 41** (2005) 1 [hep-ph/0406184] [INSPIRE].

[66] HEAVY FLAVOR AVERAGING GROUP (HFAG) collaboration, Y. Amhis et al., *Averages of b-hadron, c-hadron and τ-lepton properties as of summer 2014*, arXiv:1412.7515 [INSPIRE].

[67] Y. Sakaki and H. Tanaka, *Constraints on the charged scalar effects using the forward-backward asymmetry on $\bar{B} \to D^{(*)}\tau\bar{\nu}_\tau$*, *Phys. Rev.* **D 87** (2013) 054002 [arXiv:1205.4908] [INSPIRE].

[68] S. Fajfer, J.F. Kamenik and I. Nisandzic, *On the $B \to D^*\tau\bar{\nu}_\tau$ Sensitivity to New Physics*, *Phys. Rev.* **D 85** (2012) 094025 [arXiv:1203.2654] [INSPIRE].

[69] P. Blasi, P. Colangelo, G. Nardulli and N. Paver, *Phenomenology of B(s) decays*, *Phys. Rev.* **D 49** (1994) 238 [hep-ph/9307290] [INSPIRE].

[70] J.L. Rosner, S. Stone and R.S. Van de Water, *Leptonic decays of charged pseudoscalar mesons — 2015*, submitted to *Particle Data Book* (2015), arXiv:1509.02220 [INSPIRE].

[71] A. Bharucha, D.M. Straub and R. Zwicky, *$B \to V\ell^+\ell^-$ in the Standard Model from light-cone sum rules*, *JHEP* **08** (2016) 098 [arXiv:1503.05534] [INSPIRE].

[72] M. Dimou, J. Lyon and R. Zwicky, *Exclusive chromomagnetism in heavy-to-light FCNCs*, *Phys. Rev.* **D 87** (2013) 074008 [arXiv:1212.2242] [INSPIRE].

[73] K.-C. Yang, *Light-cone distribution amplitudes of axial-vector mesons*, *Nucl. Phys.* **B 776** (2007) 187 [arXiv:0705.0692] [INSPIRE].

[74] R. Arthur et al., *Lattice results for low moments of light meson distribution amplitudes*, *Phys. Rev.* **D 83** (2011) 074505 [arXiv:1011.5906] [INSPIRE].

[75] K.G. Chetyrkin, J.H. Kuhn and M. Steinhauser, *RunDec: a Mathematica package for running and decoupling of the strong coupling and quark masses*, *Comput. Phys. Commun.* **133** (2000) 43 [hep-ph/0004189] [INSPIRE].

[76] I. Caprini, L. Lellouch and M. Neubert, *Dispersive bounds on the shape of $\bar{B} \to D^{(*)}$ lepton anti-neutrino form-factors*, *Nucl. Phys.* **B 530** (1998) 153 [hep-ph/9712417] [INSPIRE].

[77] P. Colangelo, G. Nardulli and N. Paver, *QCD sum rules calculation of B(c) decays*, *Z. Phys.* **C 57** (1993) 43 [INSPIRE].

[78] J.A. Bailey et al., $B_s \to D_s / B \to D$ *semileptonic form-factor ratios and their application to* $BR(B_s^0 \to \mu^+\mu^-)$, *Phys. Rev.* **D 85** (2012) 114502 [*Erratum ibid.* **D 86** (2012) 039904] [arXiv:1202.6346] [INSPIRE].

[79] C. Bourrely, I. Caprini and L. Lellouch, *Model-independent description of* $B \to \pi l \nu$ *decays and a determination of* $|V_{ub}|$, *Phys. Rev.* **D 79** (2009) 013008 [*Erratum ibid.* **D 82** (2010) 099902] [arXiv:0807.2722] [INSPIRE].

[80] C.W. Bauer, D. Pirjol and I.W. Stewart, *A proof of factorization for* $B \to D\pi$, *Phys. Rev. Lett.* **87** (2001) 201806 [hep-ph/0107002] [INSPIRE].

[81] CLEO collaboration, S.E. Csorna et al., *Measurements of the branching fractions and helicity amplitudes in* $B \to D^*\rho$ *decays*, *Phys. Rev.* **D 67** (2003) 112002 [hep-ex/0301028] [INSPIRE].

[82] BELLE collaboration, R. Louvot et al., *Observation of* $B_s^0 \to D_s^{*-}\pi^+, B_s^0 \to D_s^{(*)-} rho^+$ *decays and measurement of* $B_s^0 \to D_s^{*-}\rho^+$ *polarization*, *Phys. Rev. Lett.* **104** (2010) 231801 [arXiv:1003.5312] [INSPIRE].

[83] E.E. Jenkins and M.J. Savage, *Light quark dependence of the Isgur-Wise function*, *Phys. Lett.* **B 281** (1992) 331 [INSPIRE].

[84] R.-H. Li, C.-D. Lu and Y.-M. Wang, *Exclusive* $B(s)$ *decays to the charmed mesons* $D(s) + (1968, 2317)$ *in the standard model*, *Phys. Rev.* **D 80** (2009) 014005 [arXiv:0905.3259] [INSPIRE].

[85] G. Li, F.-l. Shao and W. Wang, $B_s \to D_s(3040)$ *form factors and* B_s *decays into* $D_s(3040)$, *Phys. Rev.* **D 82** (2010) 094031 [arXiv:1008.3696] [INSPIRE].

[86] X.J. Chen, H.F. Fu, C.S. Kim and G.L. Wang, *Estimating form factors of* $B_s \to D_s^{(*)}$ *and their applications to semi-leptonic and non-leptonic decays*, *J. Phys.* **G 39** (2012) 045002 [arXiv:1106.3003] [INSPIRE].

[87] R.N. Faustov and V.O. Galkin, *Weak decays of* B_s *mesons to* D_s *mesons in the relativistic quark model*, *Phys. Rev.* **D 87** (2013) 034033 [arXiv:1212.3167] [INSPIRE].

[88] Y.-Y. Fan, W.-F. Wang and Z.-J. Xiao, *Study of* $\bar{B}_s^0 \to (D_s^+, D_s^{*+})l^-\bar{\nu}_l$ *decays in the pQCD factorization approach*, *Phys. Rev.* **D 89** (2014) 014030 [arXiv:1311.4965] [INSPIRE].

[89] M. Atoui, V. Morénas, D. Bečirevic and F. Sanfilippo, $B_s \to D_s \ell \nu_\ell$ *near zero recoil in and beyond the standard model*, *Eur. Phys. J.* **C 74** (2014) 2861 [arXiv:1310.5238] [INSPIRE].

[90] J.D. Bjorken, *Topics in B physics*, *Nucl. Phys. Proc. Suppl.* **11** (1989) 325 [INSPIRE].

[91] M. Neubert and B. Stech, *Nonleptonic weak decays of B mesons*, *Adv. Ser. Direct. High Energy Phys.* **15** (1998) 294 [hep-ph/9705292] [INSPIRE].

[92] R. Fleischer, N. Serra and N. Tuning, *A new strategy for* B_s *branching ratio measurements and the search for new physics in* $B_s^0 \to \mu^+\mu^-$, *Phys. Rev.* **D 82** (2010) 034038 [arXiv:1004.3982] [INSPIRE].

[93] LHCb collaboration, *Measurement of b-hadron production fractions in* 7 *TeV pp collisions*, *Phys. Rev.* **D 85** (2012) 032008 [arXiv:1111.2357] [INSPIRE].

[94] J.G. Korner, M. Krämer and D. Pirjol, *Heavy baryons*, *Prog. Part. Nucl. Phys.* **33** (1994) 787 [hep-ph/9406359] [INSPIRE].

[95] E. Klempt and J.-M. Richard, *Baryon spectroscopy*, *Rev. Mod. Phys.* **82** (2010) 1095 [arXiv:0901.2055] [INSPIRE].

[96] S. Meinel, *Flavor physics with* Λ_b *baryons*, PoS(LATTICE 2013)024 [arXiv:1401.2685] [INSPIRE].

[97] Y.M. Wang, *Beauty baryon decays: a theoretical overview*, *J. Phys. Conf. Ser.* **556** (2014) 012050.

[98] J.G. Korner and M. Krämer, *Exclusive nonleptonic charm baryon decays*, *Z. Phys.* **C 55** (1992) 659 [INSPIRE].

[99] H.-Y. Cheng, *Nonleptonic weak decays of bottom baryons*, *Phys. Rev.* **D 56** (1997) 2799 [hep-ph/9612223] [INSPIRE].

[100] M.A. Ivanov, J.G. Korner, V.E. Lyubovitskij and A.G. Rusetsky, *Exclusive nonleptonic decays of bottom and charm baryons in a relativistic three quark model: evaluation of nonfactorizing diagrams*, *Phys. Rev.* **D 57** (1998) 5632 [hep-ph/9709372] [INSPIRE].

[101] H.-W. Ke, X.-Q. Li and Z.-T. Wei, *Diquarks and $\Lambda_b \to \Lambda_c$ weak decays*, *Phys. Rev.* **D 77** (2008) 014020 [arXiv:0710.1927] [INSPIRE].

[102] C. Bobeth, M. Gorbahn and S. Vickers, *Weak annihilation and new physics in charmless $B \to MM$ decays*, *Eur. Phys. J.* **C 75** (2015) 340 [arXiv:1409.3252] [INSPIRE].

[103] K. Wang and G. Zhu, *Flavor dependence of annihilation parameters in QCD factorization*, *Phys. Rev.* **D 88** (2013) 014043 [arXiv:1304.7438] [INSPIRE].

[104] Q. Chang, J. Sun, Y. Yang and X. Li, *A combined fit on the annihilation corrections in $B_{u,d,s} \to PP$ decays within QCDF*, *Phys. Lett.* **B 740** (2015) 56 [arXiv:1409.2995] [INSPIRE].